CHAPTER IV

RESULTS AND DISCUSSION

In this chapter, the results are divided into four sections. The first section mainly focuses on the synthesis of ∝-bromoisobutyrate-containing silane compounds having different alkyl spacer to be used as surface-tethered initiators. The second section is devoted to the preparation and characterization of silicon-supported mixed tris(trimethylsiloxy)silyl (tris(TMS))/silanol monolayer and subsequent silicon-supported mixed tris(TMS)/∝-bromoisobutyrate monolayer which is later used as patterns for the synthesis of surface-tethered polymer brushes. The third section involves surface-initiated polymerization of 2-methacryloyloxyethyl phosphorylcholine (MPC) and *tert*-butyl methacrylate (*t*-BMA) by atom transfer radical polymerization (ATRP) from both silicon-supported ∝-bromoisobutyrate monolayer and silicon-supported mixed tris(TMS)/∝-bromoisobutyrate monolayer. The final section explains how the graft density of ∝-bromoisobutyrate groups of silicon-supported mixed tris(TMS)/∝-bromoisobutyrate monolayer influences the morphology of surface-tethered polymer brushes.
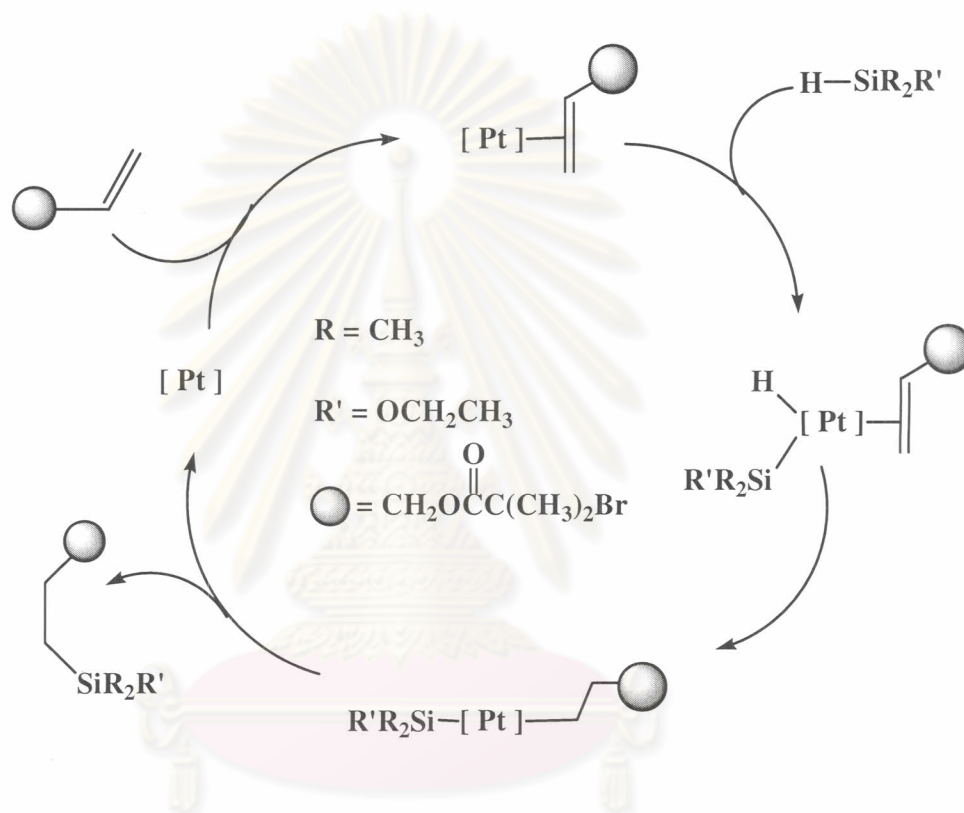
4.1 Synthesis of α-Bromoester Derivatives as Initiators

Esterification of vinyl-terminated alcohols with 2-bromoisobutyryl bromide was followed by hydrosilylation with dimethylethoxysilane to yield silane compounds having one end capable of bonding to silanol groups on silicon surface and the other end carrying latent α-bromo ester which can later be used to initiate the ATRP of vinyl monomers.

4.1.1 Synthesis of Vinyl-terminated α-Bromoisobutyrate Compounds

Three analogous vinyl-terminated alcohols (n = 3, 6, and 10) were used as substrates for this reaction. The nucleophilic acyl substitution of vinyl-terminated alcohols with 2-bromoisobutyryl bromide in tetrahydrofuran gave vinyl-terminated α-bromoisobutyrate compounds as colorless liquid products which were sufficiently pure for the next synthesis without further purification after the work-up process. The mechanism is schematically shown in Figure 4.1. The characteristic ^{1}H NMR peaks and %yield of products are listed in Table 4.1. Singlet signals of the methyl protons of C(C$\underline{H}_3$)$_2$ at 1.98, 1.90, 1.88 ppm for products **1**, **2**, and **3** represented the success of the reactions between vinyl-terminated alcohols and 2-bromoisobutyryl bromide. ^{1}H NMR spectra of product **1**, **2**, and **3** are displayed in Figures 4.3, 4.4, and 4.5, respectively.

Figure 4.1 Mechanism of nucleophilic acyl substitution of vinyl-terminated alcohol with 2-bromoisobutyryl bromide

Table 4.1 Characteristic ^{1}H NMR peaks and %yield of vinyl-terminated α-bromoisobutyrate compounds

Product No.	Name	Characteristic ^{1}H NMR peaks	% Yield
1 (n = 3)	Prop-2-enyl (2-bromo-2-methyl) propionate	singlet of C(C$\underline{H}_3$)$_2$ at 1.98 ppm	90
2 (n = 6)	Hex-5-enyl (2-bromo-2-methyl) propionate	singlet of C(C$\underline{H}_3$)$_2$ at 1.90 ppm	85
3 (n = 10)	Dec-9-enyl (2-bromo-2-methyl) propionate	singlet of C(C$\underline{H}_3$)$_2$ at 1.88 ppm	85

4.1.2 Synthesis of Silane Compounds by Hydrosilylation of Vinyl-terminated α-Bromoisobutyrate Compounds

dimethylethoxysilane   vinyl-terminated
                    α-bromoisobutyrate compounds   silane compounds

1,2,3   **4,5,6**

Hydrosilylation of dimethylethoxysilane with vinyl-terminated α-bromoisobutyrate compounds (**1**, **2**, and **3**) was carried out in the dark in the presence of chloroplatinic acid, H$_2$PtCl$_6$ at room temperature for 24 h. Figure 4.2 illustrates hydrosilylation mechanism using chloroplatinic acid as a catalyst. The reaction yielded yellow viscous liquid as a crude product which was sufficiently pure for the next synthesis without further purification after the work-up process. ^{1}H NMR spectra of the resulting silane compounds (Figures 4.3-4.5) showed methyl protons of C(C$\underline{H}_3$)$_2$ adjacent to bromine at 1.89, 1.93, 1.96 ppm for product **4**, **5**, and **6**,

respectively together with the absence of signals from two terminal protons previously appeared in vinyl-terminated α-bromoisobutyrate substrates in the range of 4-6 ppm, indicating that the reaction was successful and gave silane compounds as the desirable products.

Figure 4.2 Mechanism of hydrosilylation using chloroplatinic acid as a catalyst

Table 4.2 Characteristic ^{1}H NMR peaks and %yield of silane compounds

Product No.	Name	Characteristic ^{1}H NMR peaks	% Yield
4 (n = 3)	3 - (Dimethylethoxysilyl) propyl (2-bromo-2-methyl) propionoate	singlet of C(C$\underline{H}_3$)$_2$ at 1.89 ppm and singlet of Si(C$\underline{H}_3$)$_2$ at 0.04 ppm	93
5 (n = 6)	3 - (Dimethylethoxysilyl) hexyl (2-bromo-2-methyl) propionoate	singlet of C(C$\underline{H}_3$)$_2$ at 1.93 ppm and singlet of Si(C$\underline{H}_3$)$_2$ at 0.06 ppm	90
6 (n = 10)	3 - (Dimethylethoxysilyl) decyl (2-bromo-2-methyl) propionoate	singlet of C(C$\underline{H}_3$)$_2$ at 1.96 ppm and singlet of Si(C$\underline{H}_3$)$_2$ at 0.05 ppm	90
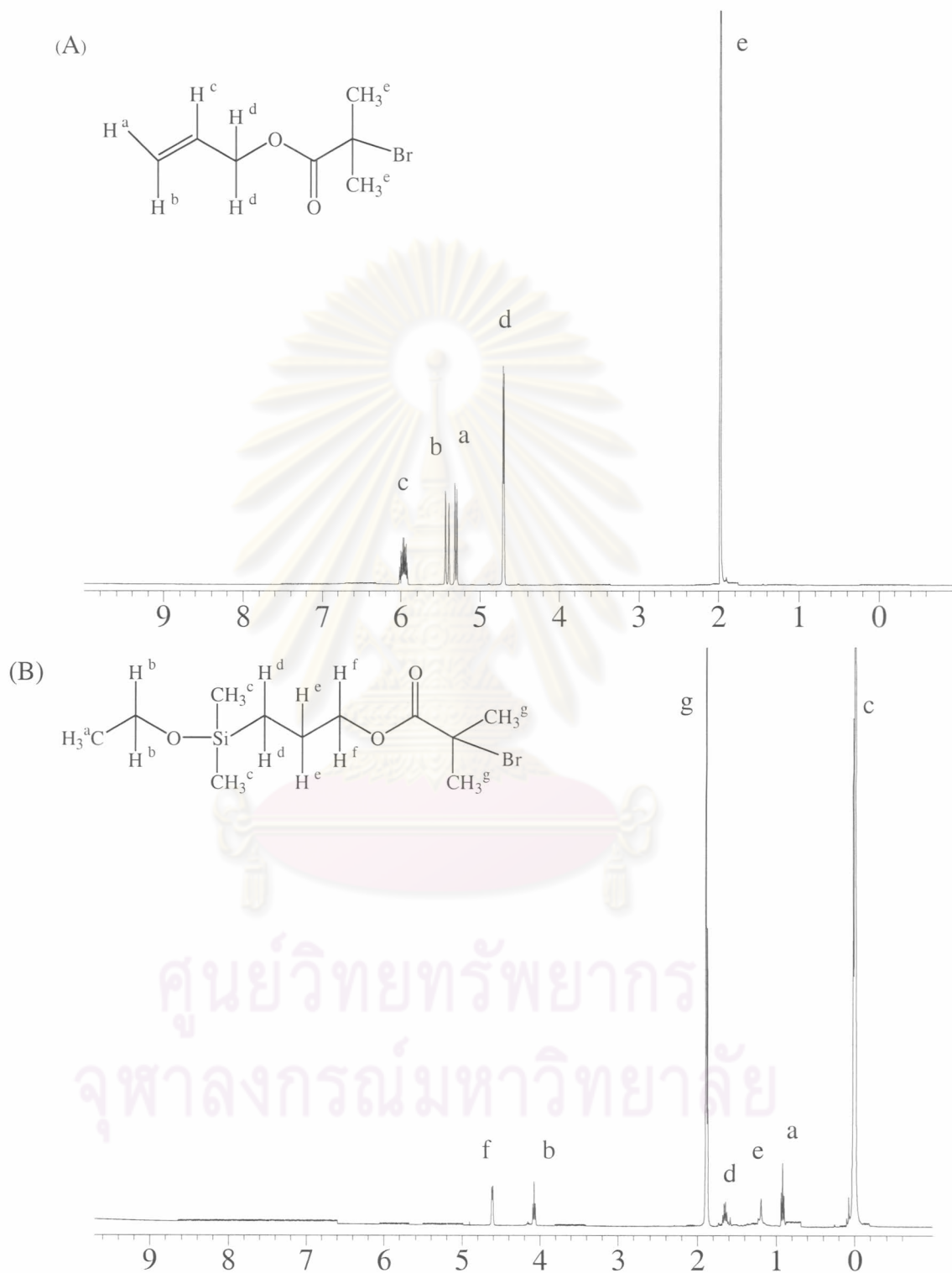
Figure 4.3 ^{1}H NMR spectra of (A) prop-2-enyl (2-bromo-2-methyl) propionate and (B) 3-(dimethylethoxysilyl) propyl (2-bromo-2-methyl) propionate.
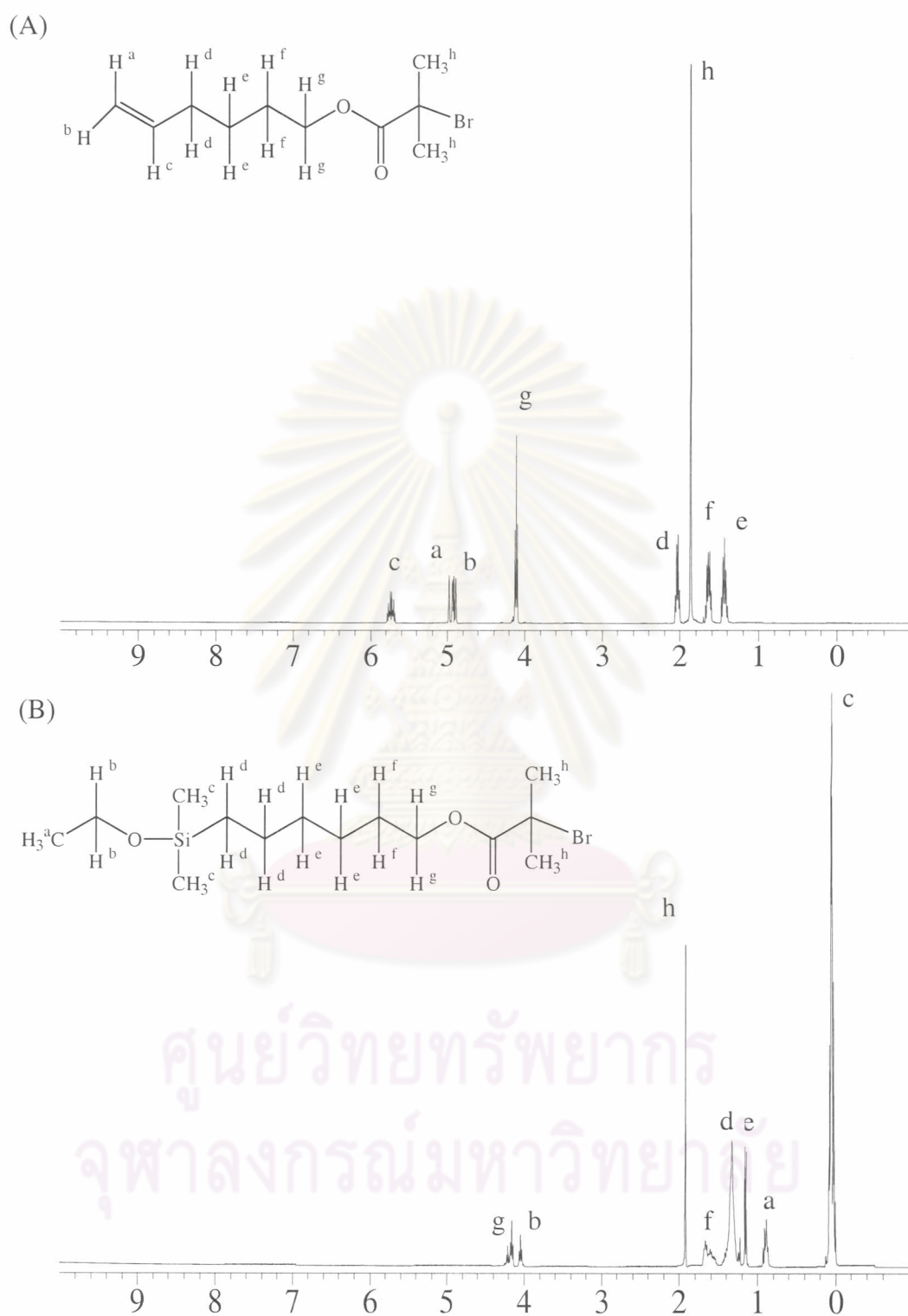
Figure 4.4 ¹H NMR spectra of (A) hex-5-enyl (2-bromo-2-methyl) propionate and (B) 3-(dimethylethoxysilyl) hexyl(2-bromo-2-methyl) propionate.

(A)

(B)

Figure 4.5 ^{1}H NMR spectra of (A) dec-9-enyl (2-bromo-2-methyl) propionate and (B) 3-(dimethylethoxysilyl) decyl (2-bromo-2-methyl) propionate.
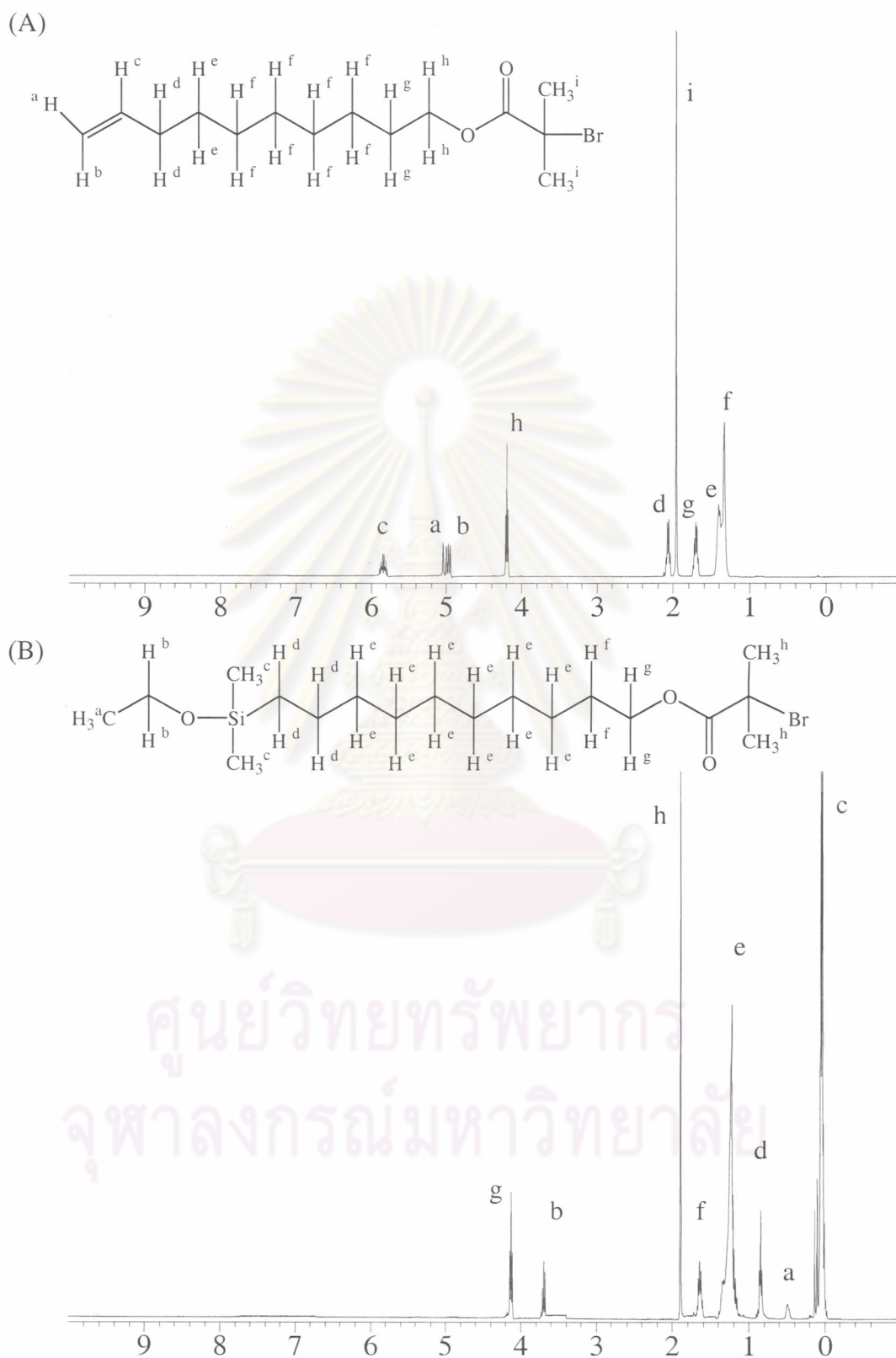
4.1.3 Synthesis of Propyl(2-bromo-2-methyl)propionate as a "Sacrificial" Initiator
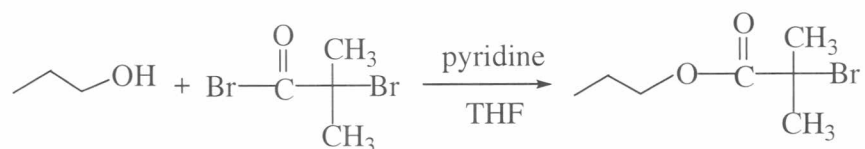
7

The nucleophilic acyl substitution of 1-propanol with 2-bromoisobutyryl bromide in tetrahydrofuran gave propyl(2-bromo-2-methyl)propionate (**7**) as a pale yellow viscous liquid (90 %yield). The ^{1}H-NMR (Figure 4.6) of product **7** showed a singlet signal of the methyl proton from C(C$\underline{H}_3$)$_2$ at 1.96 ppm indicating the success of reaction. This product was used as an "added" or "sacrificial" initiator for the polymerization of polymer brushes.
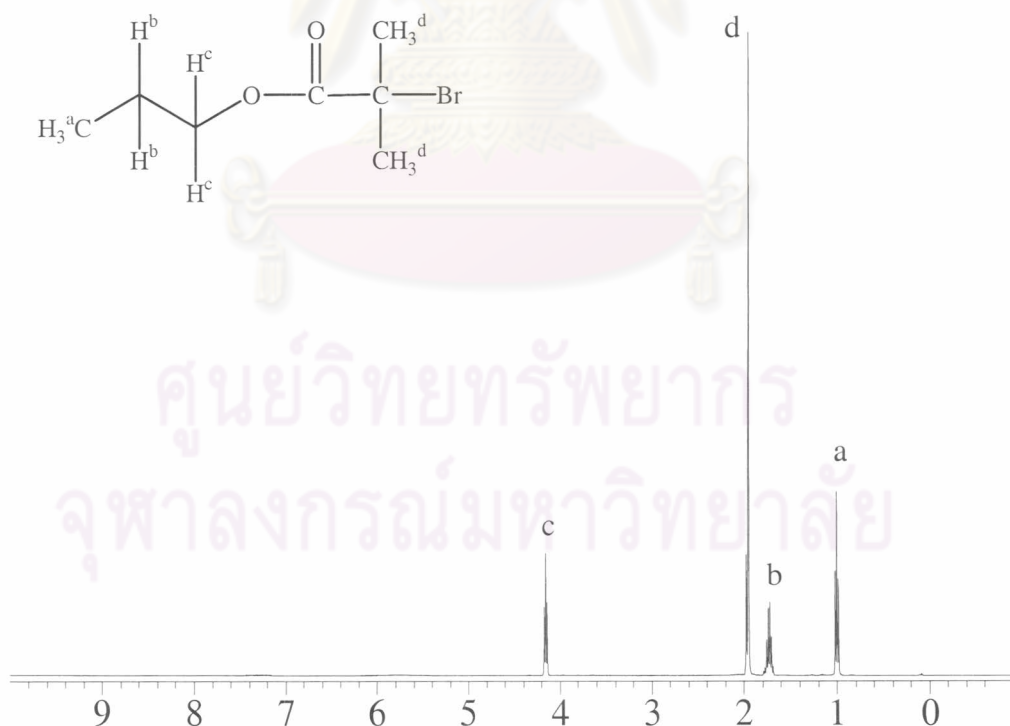
Figure 4.6 ^{1}H NMR spectrum of propyl(2-bromo-2-methyl)propionate

4.2 Preparation of Silicon -supported Mixed Tris(TMS)/silanol Monolayer

tris(TMSCl)

silicon-supported
mixed tris(TMS)/silanol monolayer
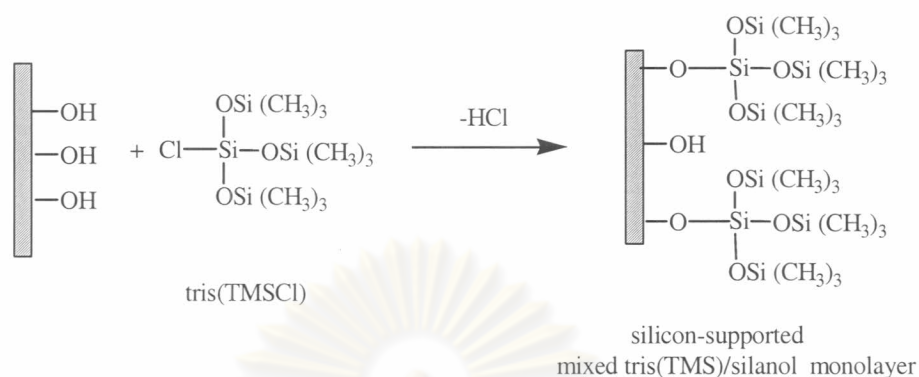
8

Monolayer of tris(trimethylsiloxy) silyl (tris(TMS)) was prepared by the reaction between tris(trimethylsiloxy) chlorosilane (tris(TMSCl)) and silanol groups on silicon substrate. By controlling the kinetics of this reaction, a series of mixed monolayer of tris(TMS)/silanol having different surface coverage of tris(TMS) can be prepared. The kinetics of reaction can be monitored by ellipsometry and contact angle analysis. As shown in Figure 4.7, ellipsometric thickness of tris(TMS) layer slowly increased as a function of reaction time and reached its maximum of ~ 20 Å after 4 days. Water contact angle data are displayed in Figure 4.8. Initially there was a rapid rise in contact angle from 29°/15° of the cleaned silicon surface to 60°/43° within 12 h, followed by a gradual increase over a period of 1-4 days, indicating that the surface became more hydrophobic as the tris-TMS coverage was increased. The contact angle of 92°/82° was eventually obtained after 4 days of reaction.
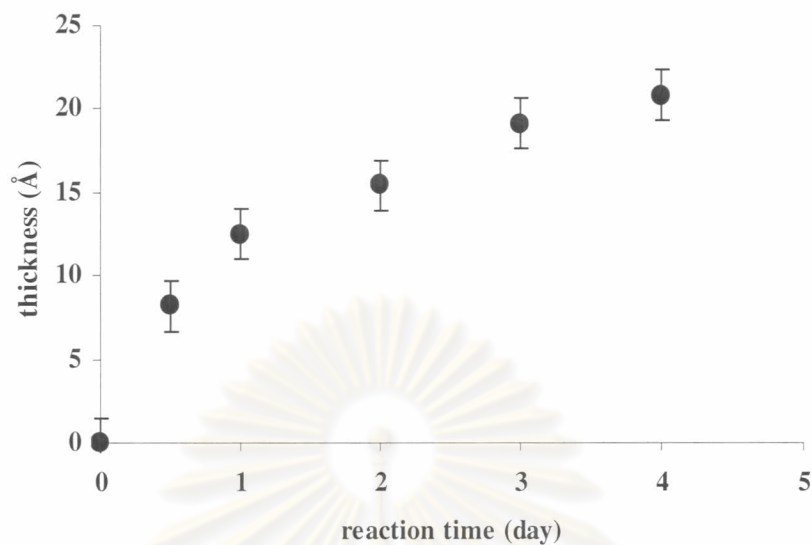
Figure 4.7 Ellipsometric thickness of tris(TMS) monolayer as a function of reaction time.
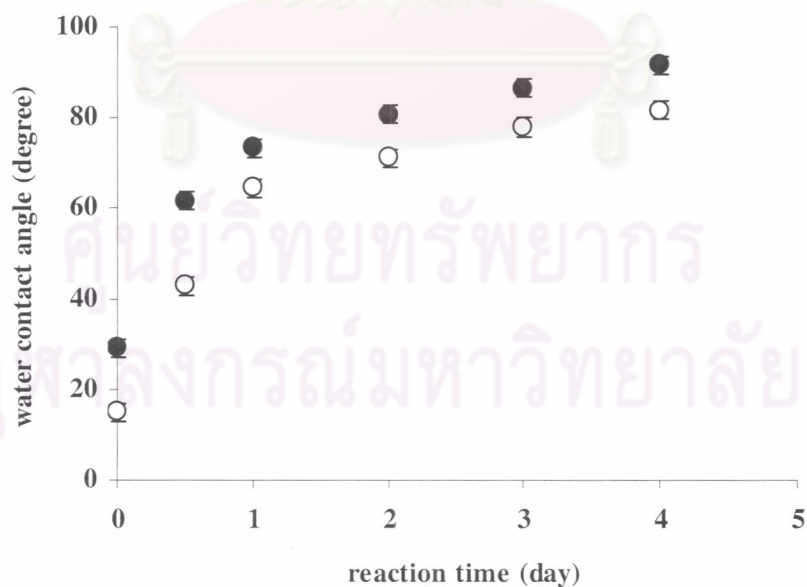
Figure 4.8 Water contact angle of tris(TMS) monolayer as a function of reaction time : advancing angle (•) and receding angle (○).

Degree of tris(TMS) coverage was determined from contact angle data according to the method proposed by Israelachvili and Gee for molecularly mixed heterogeneous surfaces [78]. The observed contact angle, θ_{obs}, can be described in terms of the mole fractions of each component, f_1 and f_2, as well as the contact angles for the pure surface of each component, θ_1 and θ_2, by

$$[1 + \cos \theta_{obs}]^2 = f_1 [1 + \cos \theta_1]^2 + f_2 [1 + \cos \theta_2]^2 \qquad (4.1)$$

$$f_1 + f_2 = 1 \qquad (4.2)$$

when θ_{obs} =   the observed advancing angle of tris(TMS) coverage

θ_1 =   the advancing angle of complete coverage of tris(TMS) monolayer ($\theta_1 = 108°$)

θ_2 =   the advancing angle of silanol monolayer ($\theta_2 = 0°$)

f_1 =   mole fraction of tris(TMS) on the surface

f_2 =   mole fraction of silanol groups on the surface

In this study, the surface was treated as a mixture of tris(TMS) groups ($\theta_1 = 108°$) and silanol groups ($\theta_2 = 0°$). It should be noted that the advancing contact angles were used for θ_{obs} in all cases. In addition, the chemical composition of the tris(TMS) monolayer was determined by XPS. The data are shown in Table 4.3 along with calculated tris(TMS) coverage and contact angles. The carbon content obviously increases as a function of reaction time, reflecting the higher degree of tris(TMS) coverage. Similar to water contact angle, the same trend was also observed when hexadecane was used as a probe fluid for contact angle measurements.

Table 4.3 XPS data (15° take-off angle), water contact angle and calculated % coverage of tris(TMS) monolayer as a function of reaction time.

Reaction time (day)	XPS atomic concentration (%)			% tris(TMS) coverage	Contact angle (θ_A / θ_R)	
	Si	O	C		water	hexadecane
0	40.50	29.75	29.75	0	29°/15°	-
0.5	-	-	-	51	62°/43°	20°/7°
1	33.66	23.26	43.08	66	73°/65°	30°/18°
2	32.96	21.25	45.79	75	81°/71°	30°/20°
3	31.29	21.39	47.32	82	86°/78°	35°/23°
4	-	-	-	87	92°/82°	34°/30°

Our results are in good agreement with that previously reported by McCarthy and coworkers [11]. As a result of bulky tris(TMS) groups, the reaction reaches its maximum extent as soon as the area occupied by unreacted silanol groups is too small for tris(TMSCl) to access. Such assumption can be supported by the fact that the contact angle tends to level off after a certain period of time (3-4 days). These residual silanol groups, not blocked by tris(TMS), are reactive sites available for adsorption or chemical reaction. McCarthy and coworkers have also demonstrated that the nanoscaled holes (nanopores) in tris(TMS) monolayer (Figure 4.9) containing unreacted silanol groups can further react with smaller silanizing reagents as well as carboxyl-functionalized polystyrene (PS-COOH) to yield binary surface mixtures [10, 11].
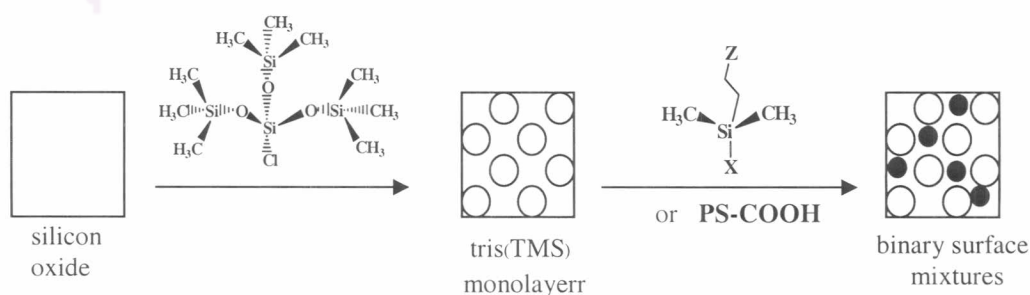
Figure 4.9 Schematic representation of nanopores in tris(TMS) monolayer

In our case, the unreacted silanol groups in the binary monolayer mixture of tris(TMS)/silanol was allowed to react with silane compounds having α-bromoester groups. The resulting binary monolayer mixture of tris(TMS)/ α-bromoester was then used as a template for surface-initiated polymerization of vinyl monomers. Detail investigation is available in the following sections.
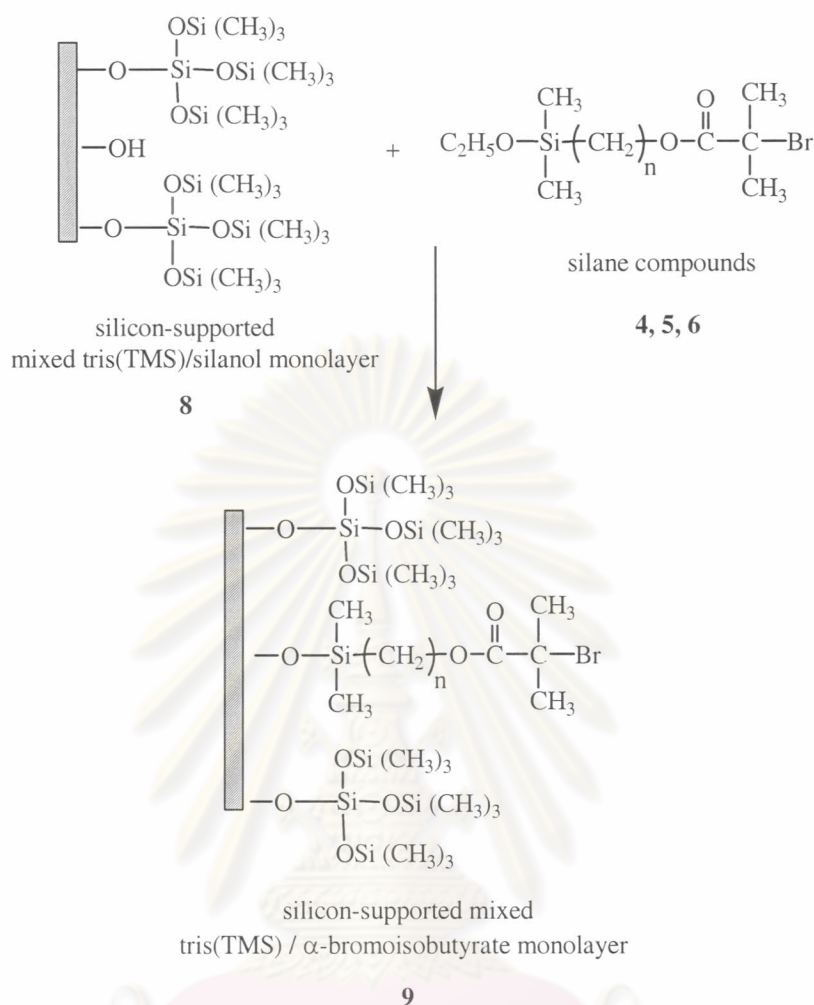
4.3 Preparation of Silicon-supported ∝-Bromoisobutyrate Monolayer and Silicon-supported Mixed Tris(TMS)/∝-Bromoisobutyrate Monolayer

silicon oxide

3-(Dimethylethoxysilyl)propyl-2-bromoisobutyrate

silicon-supported α-bromoisobutyrate monolayer
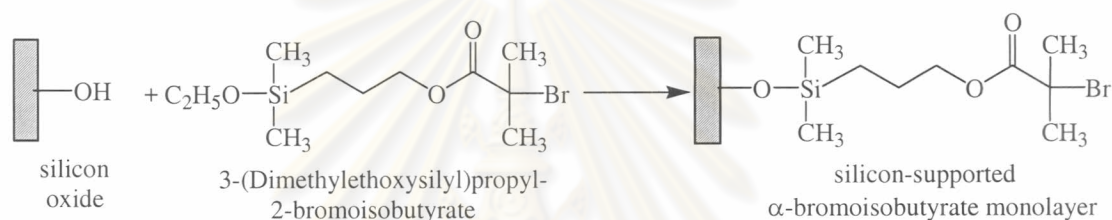
4

Using the optimized condition previously reported [70], α-bromoisobutyrate monolayer having the maximum graft density was formed on silicon substrate with a thickness 9.25 ± 0.1 Å as measured by ellipsometry. Advancing/receding water contact angle of silicon-supported ∝-bromoisobutyrate monolayer was 72°/68° which was significantly different from the value of 29°/15° for the cleaned and dried hydrophilic silicon substrates.

OSi (CH₃)₃
|
—O—Si—OSi (CH₃)₃
|
OSi (CH₃)₃

—OH   CH₃   O   CH₃
                                                        | || |
                              +   C₂H₅O—Si+CH₂)ₙ—O-C—C—Br
OSi (CH₃)₃ | |
| CH₃   CH₃
—O—Si—OSi (CH₃)₃
|
OSi (CH₃)₃

silicon-supported   silane compounds
mixed tris(TMS)/silanol monolayer

8   **4, 5, 6**

OSi (CH₃)₃
|
—O—Si—OSi (CH₃)₃
|
OSi (CH₃)₃
CH₃   O   CH₃
| || |
—O—Si+CH₂)ₙ—O-C—C—Br
| |
CH₃   CH₃

OSi (CH₃)₃
|
—O—Si—OSi (CH₃)₃
|
OSi (CH₃)₃

silicon-supported mixed
tris(TMS) / α-bromoisobutyrate monolayer

9

Silicon-supported mixed tris(TMS)/∝-bromoisobutyrate monolayers were prepared by subsequent silanization of silicon-supported mixed tris(TMS)/silanol monolayer having varied %tris(TMS) coverage with silane compounds having end-functionalized α-bromoisobutyrate(**4, 5, 6**). The silane molecules were grafted into nanopores having residual silanols in the tris(TMS) monolayers. Each silane molecule contains a bromine atom which is not present in the tris(TMS) monolayers, so the formation of silicon-supported mixed tris(TMS)/∝-bromoisobutyrate monolayers can easily be assessed by XPS analysis. These data can also be used to estimate the chemical composition of binary monolayer mixtures. XPS and contact angle data for binary monolayer mixtures of tris(TMS)/∝-bromoisobutyrate (n=3) are summarized in Table 4.4. According to contact angle analysis (data are not

shown), a period of 4 days was sufficient for the graft density of $\propto$-bromoisobutyrate groups to attain its maximum value regardless of %tris(TMS) coverage.

Table 4.4 XPS atomic composition (15° takeoff angle) and contact angle data for silicon-supported mixed tris(TMS)/$\propto$-bromoisobutyrate (n = 3) monolayer using 4 days of reaction

% tris(TMS) coverage	XPS atomic concentration (%)					Water Contact angle (θ_A / θ_R)
	Si	O	C	Br	C : Br	
0	19.37	31.24	48.52	0.87	55.8	72°/68°
66	39.49	34.25	25.87	0.39	66.3	73°/52°
75	39.97	32.84	26.82	0.37	72.5	75°/55°
82	37.66	27.31	34.57	0.46	75.1	80°/63°

As expected, the data indicated that the ratio of C:Br increased as the amount of tris(TMS) coverage increased. In another word, there are fewer $\propto$-bromoisobutyrate groups available for initiating ATRP of monomer when the content of tris(TMS) on the surface is increased. Therefore, one can use these binary monolayer mixtures of tris(TMS)/$\propto$-bromoisobutyrate as templates for controlling graft density of polymer brushes. Evidently, advancing water contact angles of silicon-supported mixed tris(TMS)/$\propto$-bromoisobutyrate monolayer was raised as a function of %tris(TMS) coverage similar to what previously observed in the case of silicon-supported mixed tris(TMS)/silanol monolayer.

4.4 Preparation of Polymer Brushes

4.4.1 Surface-initiated Polymerization of MPC from Silicon-supported α-Bromoisobutyrate Monolayer

silicon-supported
α-bromoisobutyrate monolayer

CuBr / bpy

MPC monomer

PMPC brush on silicon-supported
α-bromoisobutyrate monolayer
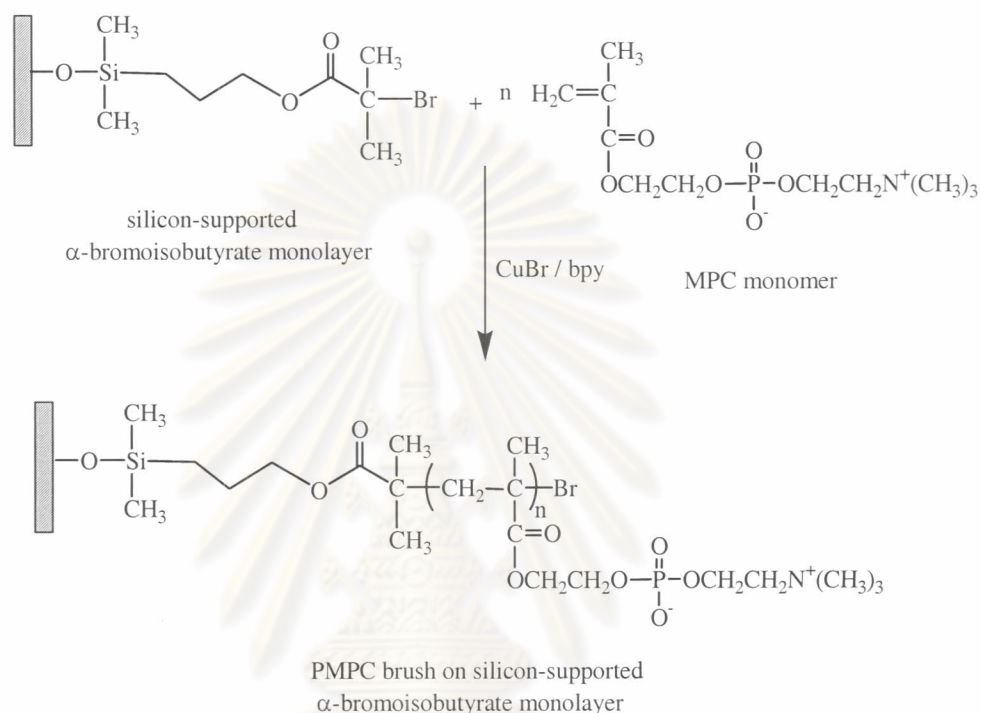
This part of research focuses on two experimental parameters that would affect the efficiency of PMPC brush growth: (1) "sacrificial" or "added" initiator and (2) deactivator. The word "sacrificial" initiator or "added" initiator represents free initiator which is not attached to the surface. It was intentionally added in the solution during surface-initiated polymerization due to 2 major reasons. The first reason is to use this free initiator (propyl(2-bromo-2-methyl)propionate in this case) to simultaneously initiate polymerization in the solution. Previous work reported by Fukuda has demonstrated that the molecular weight of this "free" polymer formed in the solution closely resembled that of the grafted polymer brushes cleaved from the surface. Thus, it can be used to monitor the surface-grafted polymerization process. [79]. The free initiator plays a role not only as an indicator of the polymerization but also as a controller for the ATRP on the surface The second reason has a lot to do with the activation/deactivation cycles of ATRP process (Figure 4.10). In the polymerization without an "added" initiator, the concentration of the Cu^{II} complex

(deactivator) produced from the reaction at the substrate surface is too low to reversibly deactivate polymer radicals with a sufficiently high rate. In the presence of an "added" initiator, the deactivator was generated by radical termination in the initial stage of polymerization until a nearly steady state concentration of copper (II) (Cu^{II}) was achieved. The "added" initiator would help increasing and adjusting the concentration of the Cu^{II} complex as in a free ATRP system. The adjustment of the Cu^{II} concentration could be made by directly adding an appropriate amount of the Cu^{II} complex which acts as a deactivator.

$$P_m\text{–}X \;+\; Cu(I)X\,/\,Ligand \;\underset{k_{deact}}{\overset{k_{act}}{\rightleftharpoons}}\; P_m^{\bullet} \;+\; X\text{-}Cu(II)X\,/\,Ligand$$

$$\overset{k_p}{(+ \; monomer)}$$

$$\xrightarrow{k_1} \quad P_m\text{—}P_n$$

Termination
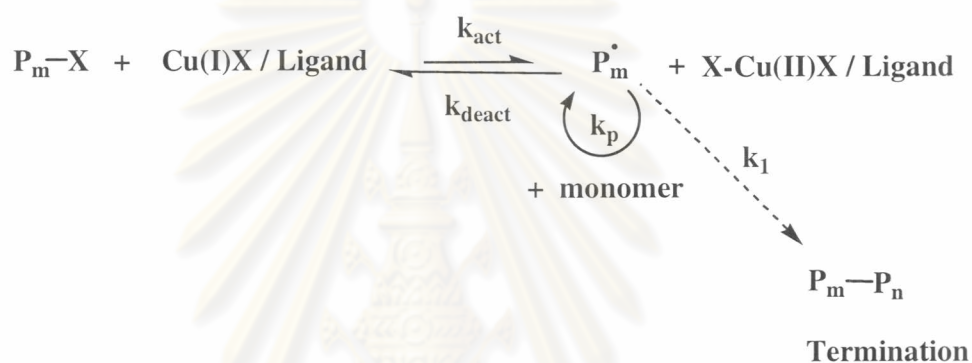
Figure 4.10 The activation/deactivation cycles of ATRP process

1) PMPC brushes prepared in the presence of "added" initiator

According to our previous work, PMPC brushes grew more rapidly in a more polar aqueous medium in comparison with a less polar alcoholic medium in the absence of "added" initiator [80]. The polar medium, especially water can facilitate the CuBr catalyst solubility and dissociation and thus accelerates the polymerization [19, 81]. Such a medium, however, deteriorated the livingness of reaction and caused premature termination as can be evidenced from the thickness of PMPC reaching a maximum value after a certain period of time. For this reason, two less polar solvent systems were selected in this study: mixed methanol:water = 4:1 (v/v) and pure methanol.

Figure 4.11 shows the development of PMPC thickness as a function of time at two targeted degrees of polymerization (DP) using the mixed methanol:water =

4:1 (v/v) as a solvent. The mole ratio of added initiator:CuBr:bpy of 1:1:2 was fixed while two mole ratios of MPC:added initiator of 50:1 and 200:1 were used. The thickness of PMPC layer increased with the increase of targeted DP. For both targeted DPs, the thickness increased linearly with time at the beginning. The rate of thickness increase of PMPC brushes seems to slow down at the later stage. This was probably due to loss of active chain ends by termination and/or diffusion limitations of monomer to the surface. This result clearly indicates that both polymerization time and [MPC]:[added initiator] ratio can be used as tools for controlling the growth of polymer brushes. The linear increase of thickness as a function of polymerization time evidently suggests that the polymerization is living in character.
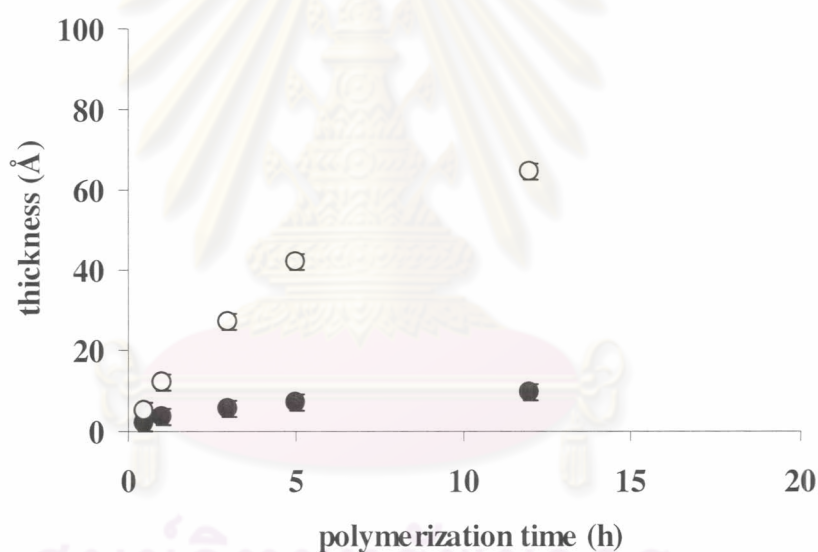
Figure 4.11 PMPC thickness versus polymerization time in the presence of "added" initiator, [MPC]:[added initiator] = 200:1 (○) and [MPC]:[added initiator] = 50:1(●) using methanol:water = 4 : 1 (v/v) as a solvent.

Under the same condition to obtain the targeted DP of 200, PMPC brushes prepared in pure methanol was relatively thinner than those prepared in mixed methanol/water. The relationships between PMPC brush thickness prepared in pure methanol and the one prepared in mixed methanol/water and reaction time are shown in Figure 4.12. As explained earlier by Armes and coworkers [82], the presence of

water in the mixed solvent helps increase the solubility of the catalyst as well as increase the activation rate constant (k_{act}) in ATRP. In addition, in more polar media, the bromide anion is sufficiently stable and well solvated, resulting in $Cu(bpy)_2^+ Br^-$ species. While, in less polar media, Br^- is destabilized and concurrently binds much stronger to CuBr than bpy does, resulting in $Cu(bpy)_2^+ CuBr_2^-$ species. These results agree very well with the previous data [30]. In spite of the variation in thickness of PMPC brushes, good control over the growth of PMPC brushes can be achieved using both mixed methanol:water (4:1 v/v) and pure methanol.
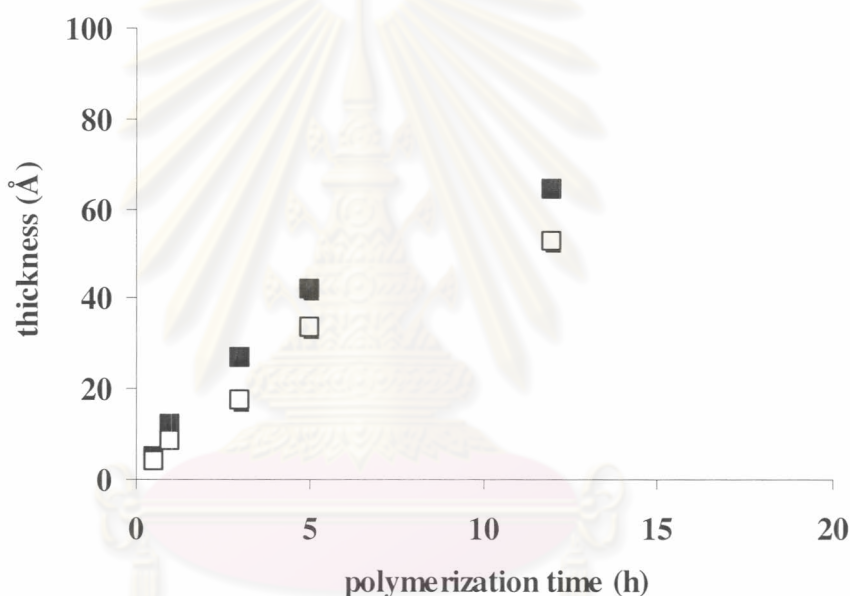
Figure 4.12 Ellipsometric thickness of PMPC brushes versus polymerization time for targeted DP = 200 in methanol:water = 4 : 1 (v/v) (■) and pure methanol (□).

The growth of PMPC brushes can also be monitored by water contact angle analysis. Figure 4.13 shows advancing (θ_A) and receding (θ_R) water contact angles of silicon-supported PMPC brushes as a function of polymerization time. Both advancing and receding contact angles rapidly dropped with time from $72°/68°$ of the hydrophobic silicon-supported α-bromoisobutyrate monolayer (n = 3) to ~ $20°/1°$ of the hydrophilic silicon-supported PMPC brushes after 1 h of reaction. The contact

angle data also imply that the surface bearing PMPC brushes is quite homogeneous and smooth. The independence of water contact angle on the thickness of PMPC brushes evidently suggests that the growing of each polymer brush is simultaneous and living in character.
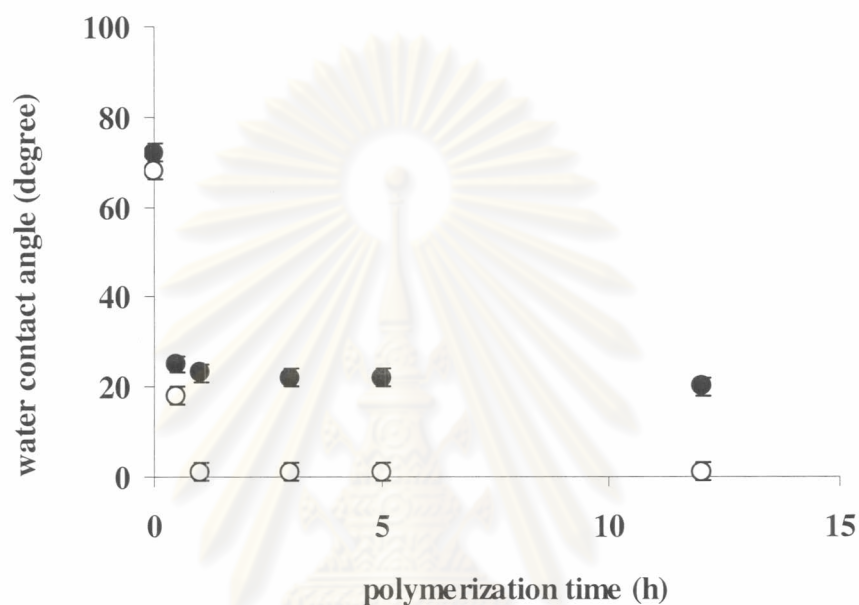
**Figure 4.13** Water contact angle data of PMPC brushes versus polymerization time for targeted DP = 200 using methanol/water = 4:1 (v/v) as a solvent: θ_a (●) and θ_r (○).

The receding angle was re-plotted together with ellipsometric thickness of PMPC brushes (Figure 4.14) in order to demonstrate that the wetting has reached its equilibrium at relatively low thickness (~10 Å). Despite the slightly thinner layer of PMPC brushes, a similar trend was also observed in Figure 4.15 when pure methanol was used as a solvent.
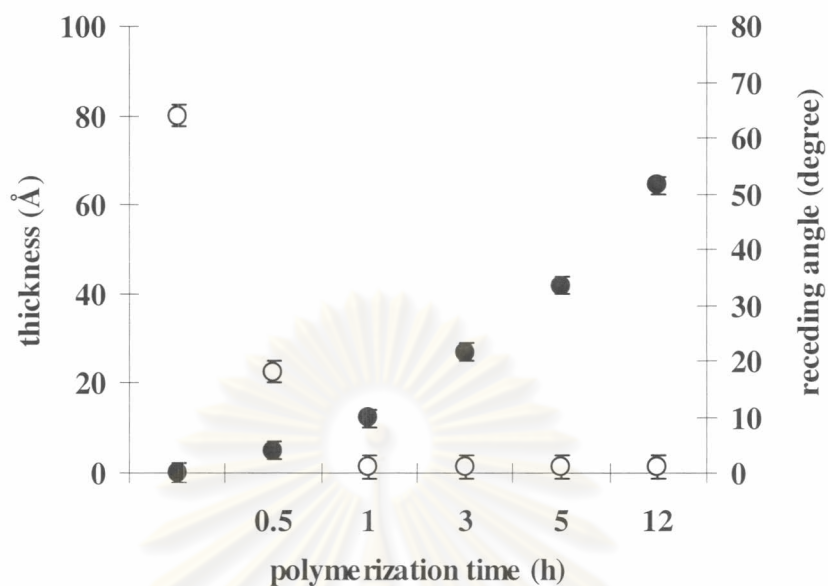
Figure 4.14 Ellipsometric thickness (●) and receding water contact angle (θ_r) (○) of PMPC brushes versus polymerization time for targeted DP = 200 using methanol:water = 4:1 (v/v) as a solvent
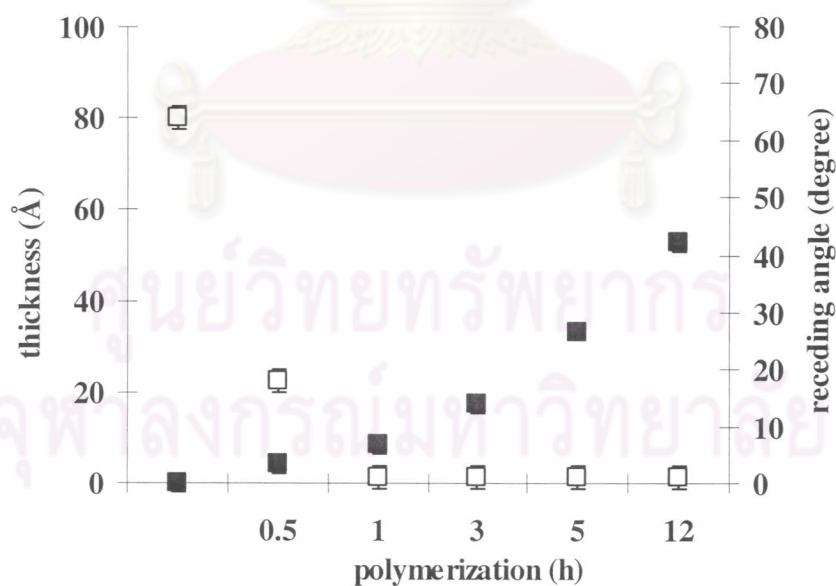
Figure 4.15 Ellipsometric thickness (■) and receding water contact angle (θ_r) (□) of PMPC brushes versus polymerization time for targeted DP = 200 using methanol as a solvent

2)PMPC brushes prepared in the presence of deactivator

Although the addition of "added" initiator is strongly recommended by many research groups as an effective method to control the growth of polymer brushes, some of them have argued that such method generates a large quantity of free polymer formed in the solution. This free polymer as a side product of polymer brush formation somewhat leads to the tedious process of surface cleaning after reaction.

To overcome this disadvantage, an alternative approach of adding an deactivator has been proposed. In this research, $CuBr_2$ was added in the solution to generate Cu(II) which can act as the deactivator in the absence of "added" initiator. Figure 4.16 illustrates the development of thickness of PMPC brushes using different mole ratio of $CuBr:CuBr_2$ (1:0, 1:0.1 and 1:0.5) and [MPC] = 0.012 mole. In the absence of $CuBr_2$, the thickness increased rapidly in the early stage and level off after a certain period of time indicating that the polymerization was not well controlled. This can be explained by the fact that the concentration of the Cu^{II} complex (deactivator) produced from the reaction at the substrate surface is too low to reversibly deactivate polymer radicals with a sufficiently high rate. The radicals on the surface once generated could not easily revert with the dormant state, and thus participated in side reactions leading to the loss of active chains. The major side reaction on the surface was bimolecular termination. Adding 10 mol% $CuBr_2$ ($CuBr:CuBr_2$ =1:0.1) to the system decreased the initial polymerization rate. The reduced rate was caused by lower radical concentration on the surface due to the added $CuBr_2$ that deactivated the radicals. The thickness of PMPC brushes linearly increased as a function of polymerization time suggesting that polymerization is living and can be well controlled. Increasing the $CuBr_2$ concentration to 50 mol% ($CuBr:CuBr_2$ =1:0.5) minimized side reactions of the radicals at the surface, but decreased the rate of polymerization significantly. This outcome indicate that only small amount of $CuBr_2$ is necessary for balancing activation / deactivation cycle of ATRP.
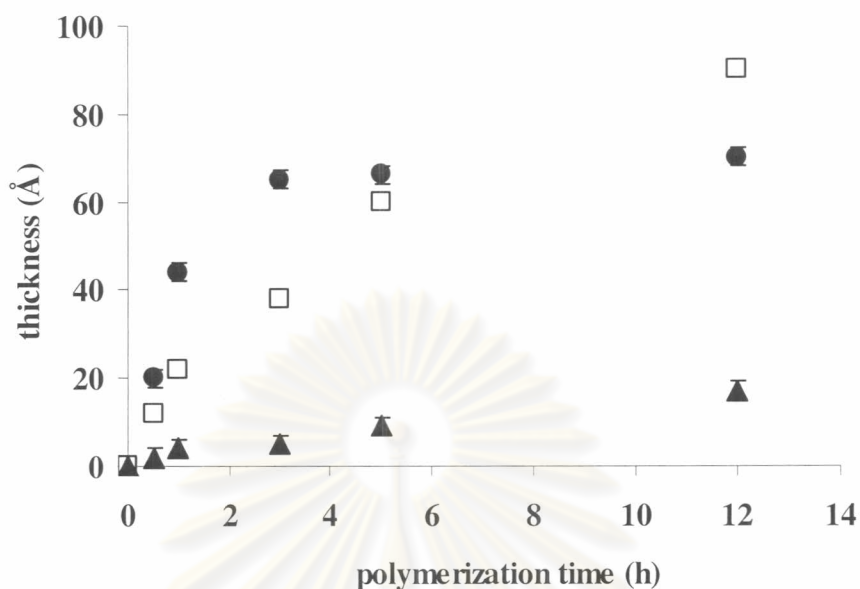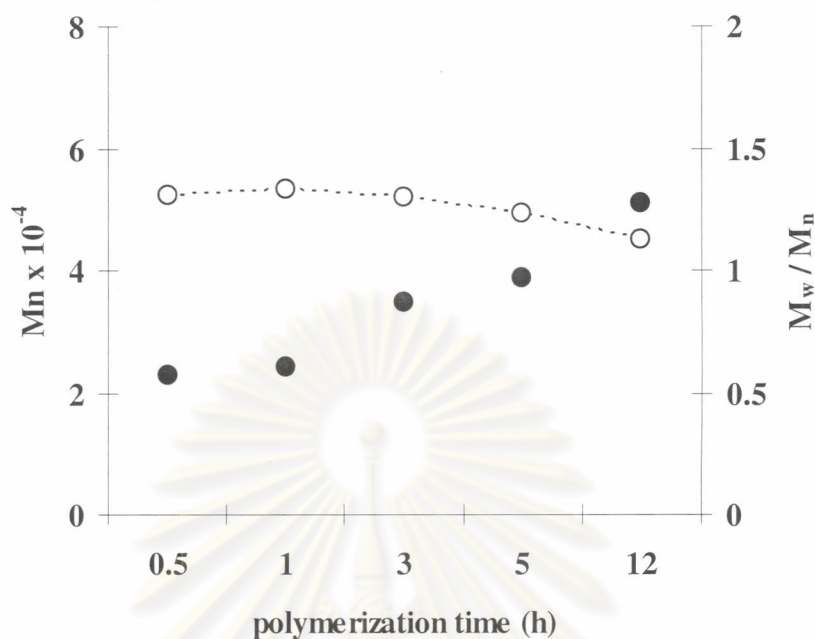
Figure 4.16 Ellipsometric thickness of PMPC brushes versus polymerization time for different [CuBr]/[CuBr$_2$] ratios at targeted DP of 200 using methanol:water = 4:1 (v/v) as a solvent: [CuBr]/[CuBr$_2$] = 1:0 (●), 1:0.1 (□) and 1:0.5 (▲).

### 3) Molecular Weight and Graft Density of PMPC brushes

It is rather difficult to obtain the molecular weight of the polymer brush directly since the amount of polymer on the silicon wafer is too small to degraft and analyze. The information related to molecular weight distribution and molecular weight which can be used to calculate the graft density of polymer brushes can thus be obtained from the "free" polymer chains formed by the "added" initiator in solution. Figure 4.17 shows the change in the molecular weight ($\overline{M}_w$) and molecular weight distribution ($\overline{M}_w/\overline{M}_n$) of free PMPC produced in methanol:water = 4:1 (v/v) as a function of polymerization time. The molecular weight increased linearly with increasing polymerization time. The molecular weight distribution being close to 1.0 suggested that polymerization mechanism is living.

Figure 4.17 The molecular weight ($\overline{M}_n$) (●) and molecular weight distribution ($\overline{M}_w/\overline{M}_n$) (○) of free PMPC for targeted DP = 200 produced in methanol:water = 4:1 (v/v) as a function of polymerization time.

Figures 4.18 and 4.19 show the ellipsometric thickness of grafted PMPC brushes versus the molecular weight ($\overline{M}_n$) of PMPC formed in solution that was produced by the free initiator. A linear relationship was observed for both targeted DPs, demonstrating a good control of the grafting process with the added free initiator. The thickness at the targeted DP = 200 were almost a factor of four greater than those at the targeted DP = 50.
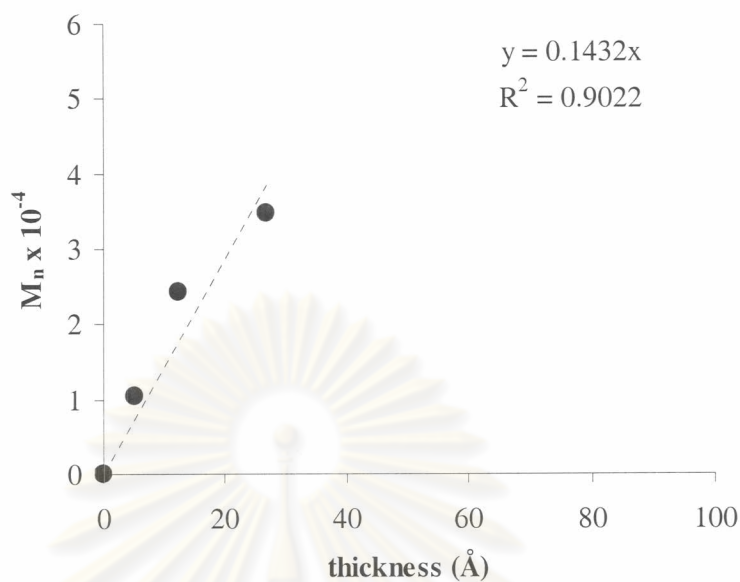
Figure 4.18 Relationship between the ellipsometric thickness of PMPC brushes with the molecular weight ($\overline{M}_n$) of free PMPC for targeted DP = 200 produced in methanol:water = 4:1 (v/v).
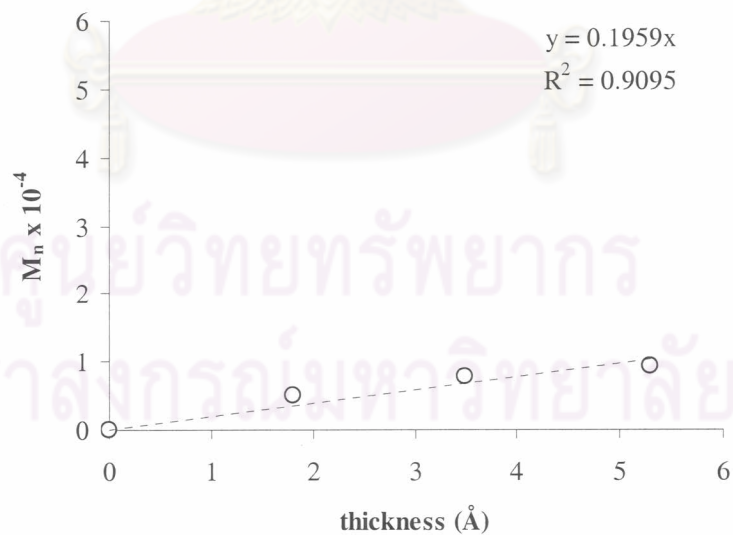
Figure 4.19 Relationship between the thickness of PMPC brushes with the molecular weight ($\overline{M}_n$) of free PMPC for targeted DP = 50 produced in methanol:water = 4:1 (v/v).

Graft density (σ) which is a unit per cross-sectional area (A_x) per chain can be determined from the corresponding film thickness (t) and the molecular weight of the chain (M) from the following equation:

$$\sigma = \frac{t\rho\, N_A}{M} = \frac{1}{A_x} \qquad (4.3)$$

Where ρ is the mass density (1.30 g/cm^3 for PMPC) [84] and N_A is Avogadro's number. Using slopes obtained from the plots in Figures 4.18 and 4.19 which correspond to M/t, calculated grafting densities are 0.46 and 0.34 chains/nm^2 for the targeted DP = 200 and targeted DP = 50, respectively. These results agree quite well with the data previously reported that the graft densities for various polymers prepared by surface-initiated ATRP were also ranged from 0.1 to 0.6 chains/nm^2 [83]. Feng and coworkers [71] also reported grafting densities of PMPC brushes as 0.32 and 0.28 chains/nm^2 for the targeted DP = 200 and targeted DP = 50, respectively.

4) Confirmation of PMPC brushes by XPS

XPS was used to confirm the formation of the initiator monolayer and the growth of PMPC brushes. The data are outlined in Table 4.5. The α-bromoester layer was indicated by the signal of Br_{3d}. The N_{1s} and P_{2p} data suggested that phosphatidylcholine analogous groups were present on the surface after the formation of PMPC brushes. The N/P ratio at 15° of take-off angle of ~ 0.8 reasonably agreed with the stoichiometric ratio of MPC unit. Due to partial X-ray damage of bromine during XPS analysis along with the fact that bromine may be buried within the polymer brushes when the brushes were relatively thick [85], the percentage of Br_{3d} was neither quantitative nor consistent with the percentages of N_{1s} and P_{2p}.

Table 4.5 XPS atomic composition (%) of silicon surfaces before and after the formation of PMPC brushes.

Surface	Atomic Composition (%)					
	Si	C	O	Br	P	N
Silicon	40.50	29.75	29.75	-	-	-
α-bromoester	19.37	48.52	31.24	0.87	-	-
PMPC brushes	16.52	48.97	32.38	0.00	1.16	0.96
(thickness = 64 Å)						

4.4.2 Surface-initiated Polymerization of *t*-BMA from Silicon-supported α-Bromoisobutyrate Monolayer

silicon supported
α-bromoisobutyrate monolayer

t-BMA monomer

CuBr/PMDETA

P*t*-BMA brush on silicon-supported
α-bromoisobutyrate monolayer
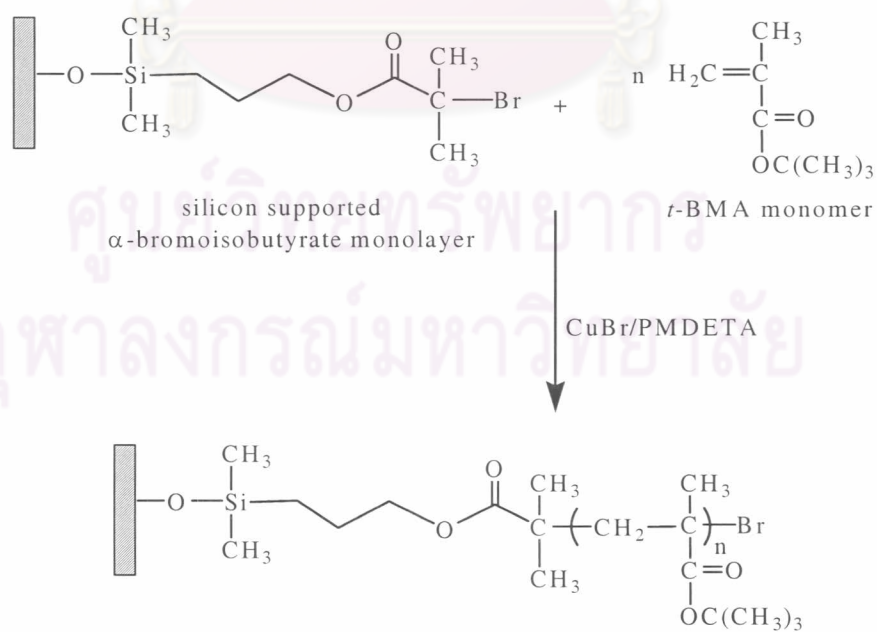
P*t*-BMA brushes were grown from the surface bearing α–bromoisobutyrate monolayer *via* ATRP mechanism in the presence of CuBr/PMDETA using toluene as a solvent. The polymerization was conducted at 90°C. The CuBr/PMDETA catalyst system was used in the homogeneous and heterogeneous metal-catalyzed living radical polymerization of *tert*-butyl methacrylate (*t*-BMA). PMDETA was selected because the catalyst complex is (i) highly active, (ii) easily available, (iii) cost-effective and (iv) can be easily separated from the polymer [86]. Propyl(2-bromo-2-methyl)propionate was also used as a "free" initiator.

Figure 4.20 shows the relationship between thickness of P*t*-BMA brushes growing from the α–bromoisobutyrate monolayer and polymerization time. For targeted DP = 200, it was found that the thickness of P*t*-BMA brushes increased with increasing polymerization time similar to what previously observed in the case of PMPC brushes. The growth of P*t*-BMA brushes can also be monitored by water contact angle analysis. Figure 4.21 illustrates advancing (θ_A) and receding (θ_R) water contact angles of silicon-supported P*t*-BMA brushes as a function of polymerization time. Both advancing and receding contact angles rapidly increased from $72^\circ/68^\circ$ of silicon-supported α-bromoisobutyrate monolayer (n = 3) to ~ $90^\circ/70^\circ$ of a more hydrophobic silicon-supported P*t*-BMA brushes. The contact angle data also imply that the surface bearing P*t*-BMA brushes is quite homogeneous and smooth.
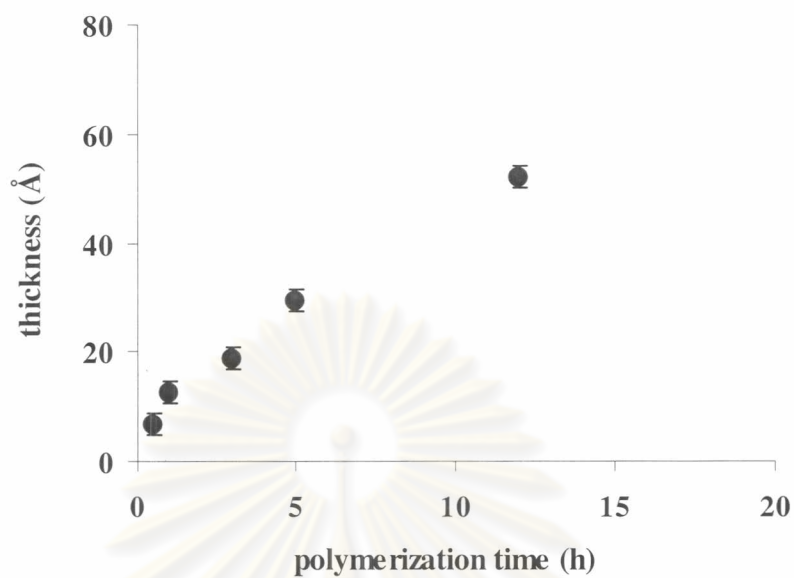
Figure 4.20 Ellipsometric thickness of P*t*-BMA brushes versus polymerization time
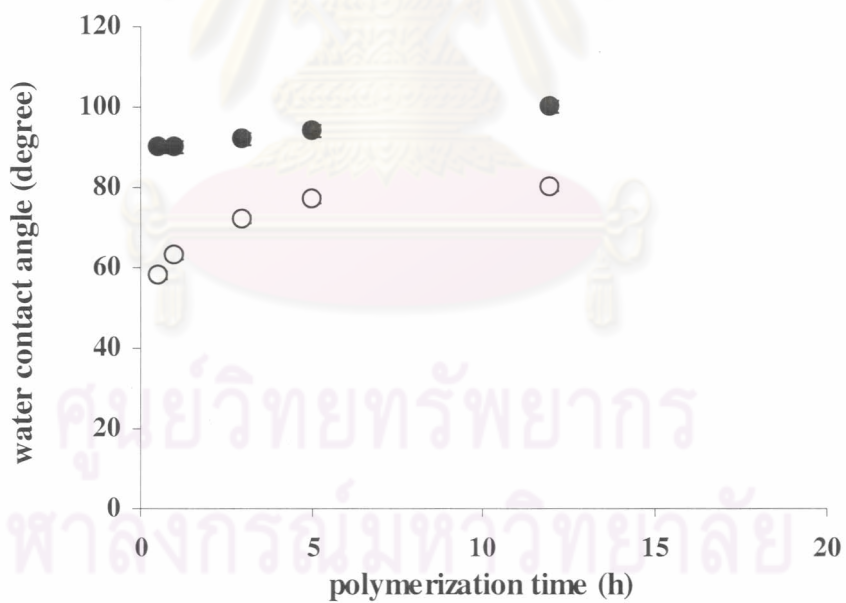
Figure 4.21 Water contact angle data of P*t*-BMA brushes versus polymerization time for targeted DP = 200: θ_A (●) and θ_R (○).

Figure 4.22 shows that the ellipsometric thickness of grafted Pt-BMA brushes versus the molecular weight ($\overline{M}_n$) of Pt-BMA formed in solution that was produced by the free initiator. Using equation 4.3 and M/t (obtained from the slope of graph in Figure 4.22 and the mass density 1.10 g/cm^3 [85]), Graft density of Pt-BMA brushes for the targeted DP of was equal to 0.25.

$$y = 0.2581x$$
$$R^2 = 0.9673$$
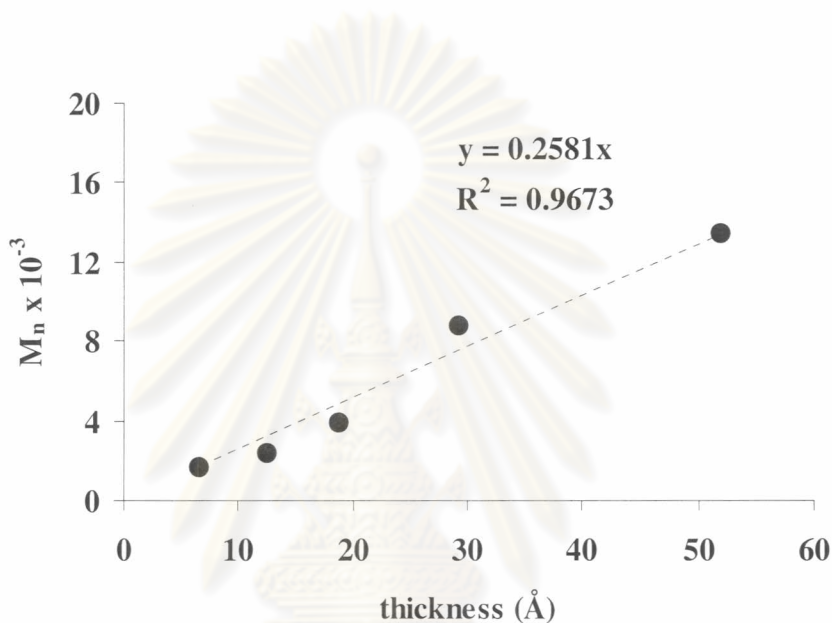
Figure 4.22 Relationship between the thickness of Pt-BMA brushes with the molecular weight ($\overline{M}_n$) of free Pt-BMA for targeted DP = 200 produced in toluene at 90 °C.

Figure 4.23 shows the change in the molecular weight ($\overline{M}_n$) and molecular weight distribution ($\overline{M}_w/\overline{M}_n$) of free P$t$-BMA as a function of polymerization time. The molecular weight increased linearly with increasing polymerization time. The molecular weight distribution being close to 1.0 suggested that polymerization mechanism is living.
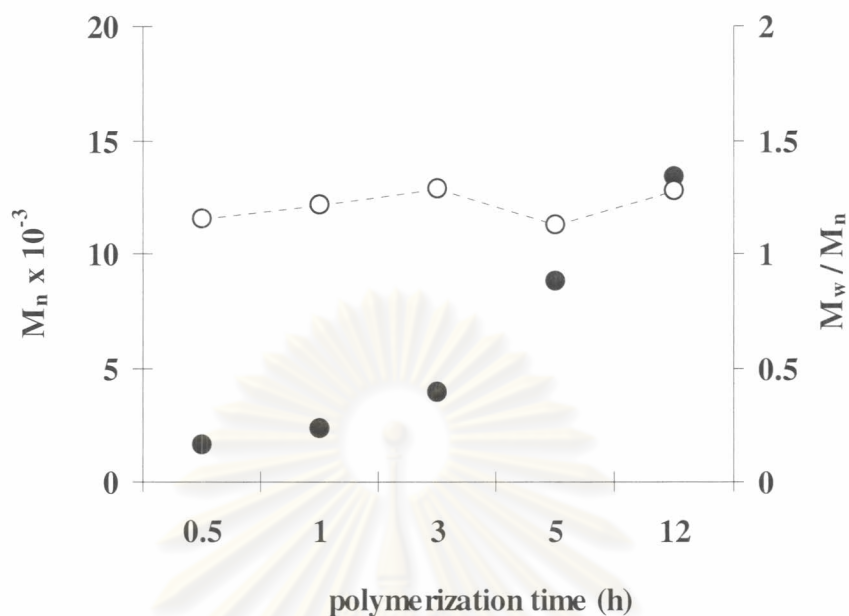
Figure 4.23 The molecular weight $(\overline{M}_n)$ (●) and molecular weight distribution $(\overline{M}_w/\overline{M}_n)$ (○) of free Pt-BMA for the targeted DP = 200 produced in toluene at 90°C as a function of polymerization time.
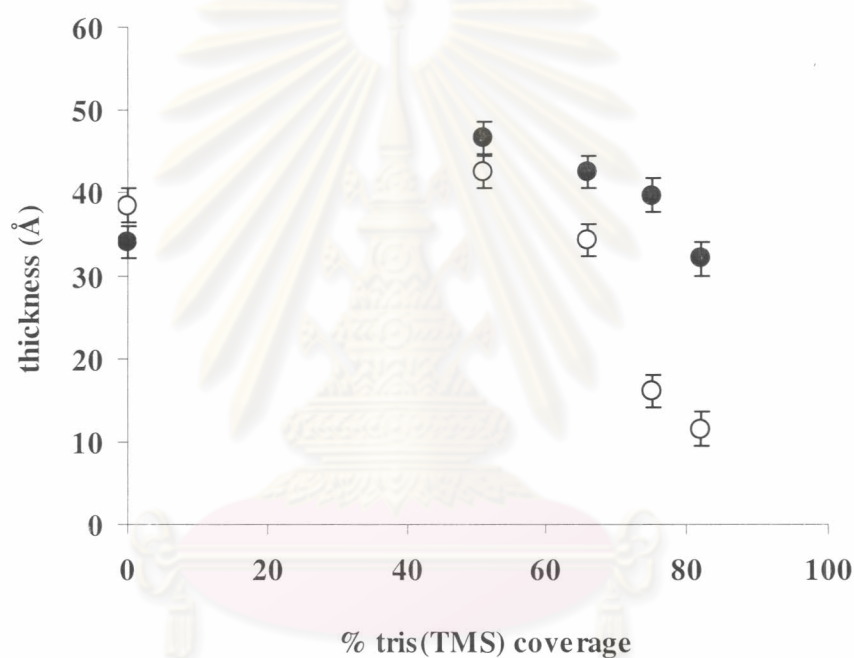
4.4.3 Surface-initiated Polymerization of MPC from Silicon-supported Mixed Tris(TMS)/∝-Bromoisobutyrate Monolayer

silicon-supported mixed
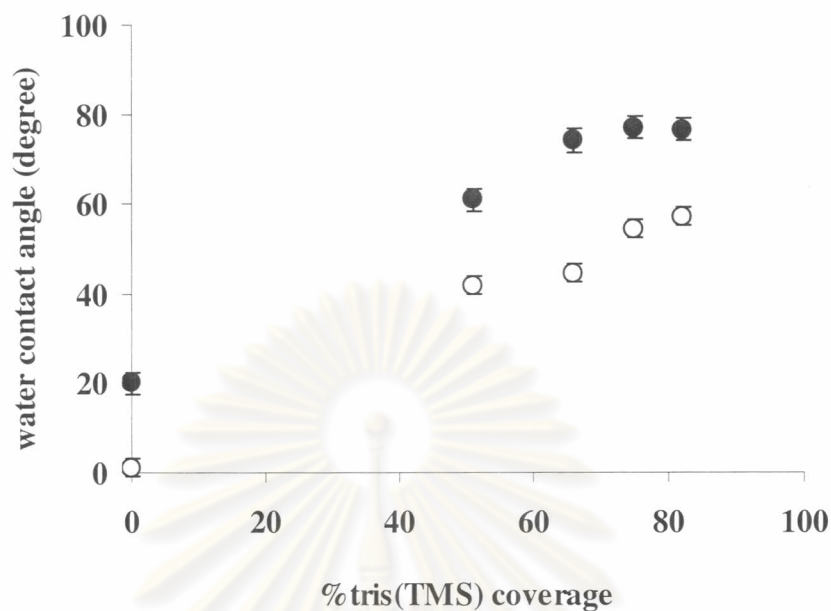tris(TMS) / α-bromoisobutyrate monolayer

9

CuBr/bpy

MPC monomer

PMPC brush on silicon-supported
mixed tris(TMS) / α-bromoisobutyrate monolayer
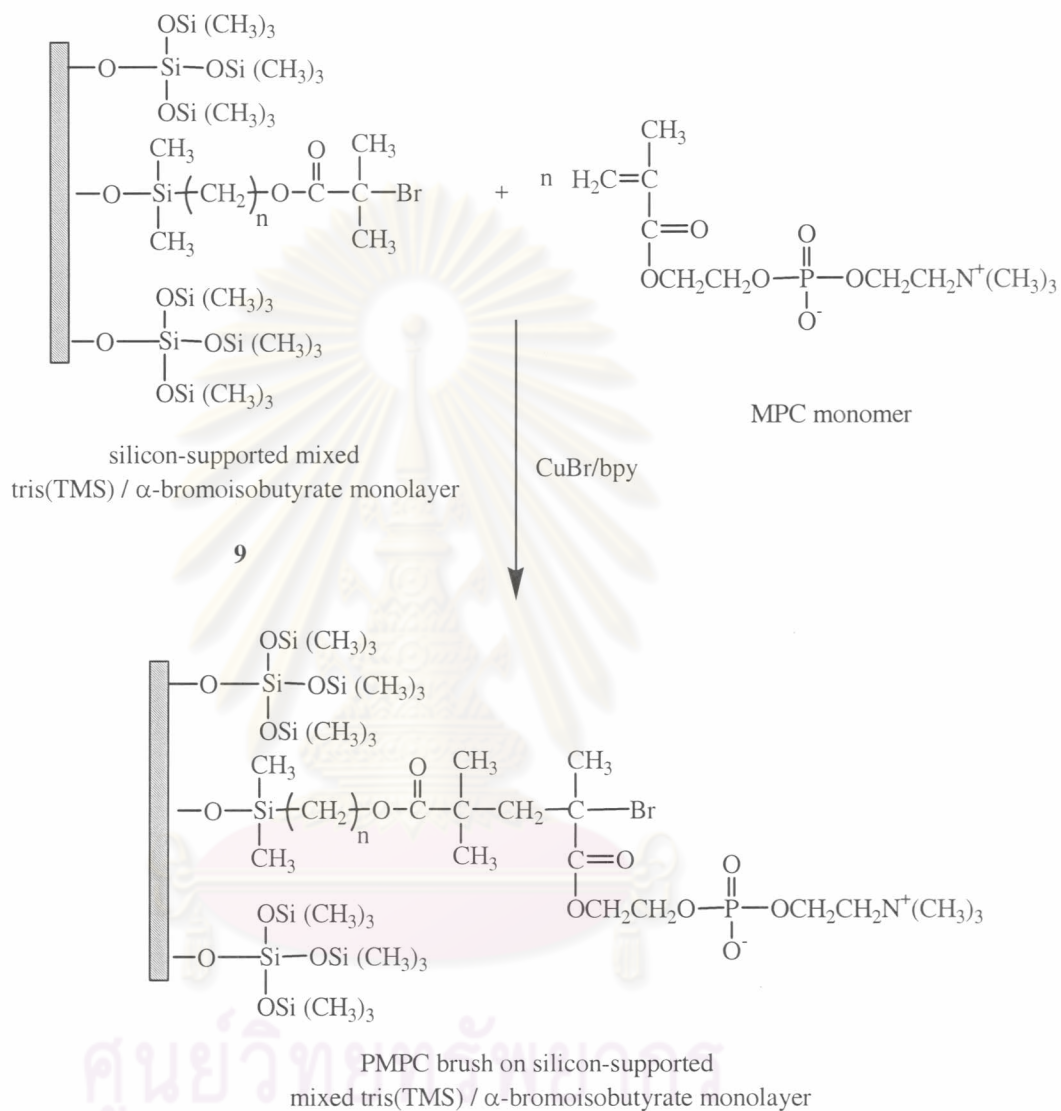
As mentioned earlier, silicon-supported mixed tris(TMS)/∝-bromoisobutyrate monolayer was intended to be used as nanoscaled templates for the formation of PMPC brushes. In this section, the growth of PMPC brushes as a function of %tris(TMS) coverage, the type of grafted α-bromoisobutyrate and polymerization time are primarily discussed in terms of water contact angle and ellipsometric thickness. The results from morphological studies of silicon-supported polymer brushes are separately provided in section 4.5.

As demonstrated in Figure 4.24, the thickness of PMPC brushes which corresponded with the density and length of polymer brushes decreased as the % tris(TMS) coverage increased. Due to the hydrophobicity of tris(TMS) groups surrounding $\propto$-bromoester initiators, the growth of polymer brush is more favorable in a more surface-wettable solvent, methanol in this particular case, than water. Using 5h of polymerization, PMPC brushes prepared in methanol are relatively thicker than those obtained in water.

Figure 4.24 Ellipsometric thickness of PMPC brushes grown from silicon-supported mixed tris(TMS)/$\propto$-bromoisobutyrate monolayer using methanol (●) or water (○) as a solvent.

The advancing and receding angles of PMPC brushes on the mixed tris(TMS)/$\propto$-bromoisobutyrate increased with increasing % tris(TMS) coverage. Relatively high advancing angles reflect the assumption that tris(TMS) groups dominate at the polymer/air interfaces. Receding angles can better represent how hydrophilic the mixed surface is.

Figure 4.25 Water contact angle of PMPC brushes grown from silicon-supported mixed tris(TMS)/∝-bromoisobutyrate monolayer using methanol as a solvent for 5 h: θ_A (●) and θ_R (○).

The growth of PMPC brushes from nanopores can also be tuned by polymerization time. Figure 4.26 shows the thickness and receding water contact angle of the silicon-supported tris(TMS)/PMPC brushes having 82% tris(TMS) coverage as a function of polymerization time. The longer the polymerization proceeds, the thicker the polymer brush and the more hydrophilic the surface becomes.
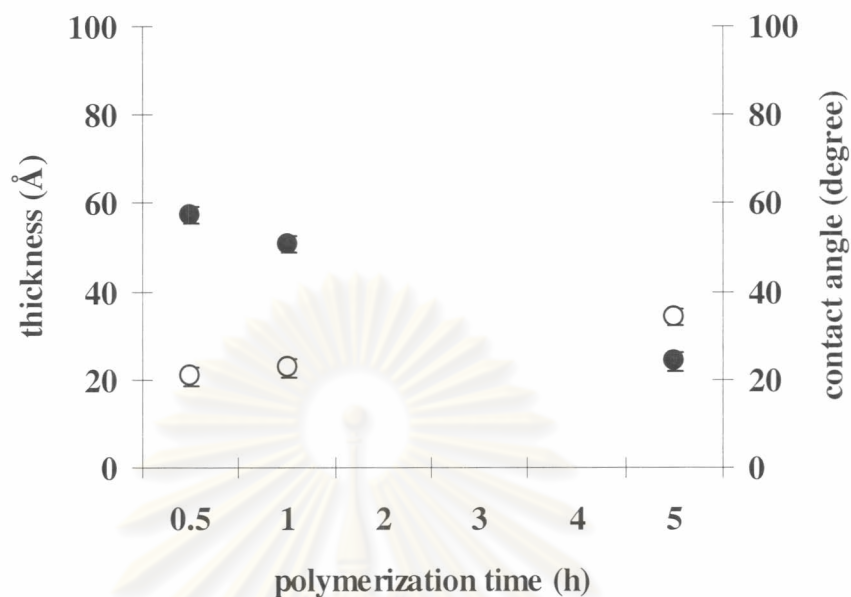
Figure 4.26 Ellipsometric thickness (○) and receding water contact angle (●) of silicon-supported mixed tris(TMS)/PMPC brushes having 82% tris(TMS) coverage as a function of polymerization time.

Originally, the fact that the surface having a certain %tris(TMS) coverage (~15-20 Å) is relatively thicker than α-bromoisobutyrate monolayer (~10 Å) brought a concern that the short alkyl chain, especially for the silane having n=3 might be buried in the nanopores surrounded by tris(TMS) and unable to initiate polymerization. Therefore, three analogous series of silane compounds having end-functionalized α-bromoisobutyrate groups were used to react with residual silanols in nanopores in order to determine the effect of alkyl spacer (n = 3, 6, and 10) between the surface-immobilized end and the other end bearing α-bromoisobutyrate group on the efficiency to initiate polymerization. The immobilized α-bromoisobutyrate initiator is defined according to its alkyl spacer as n_3, n_6, and n_{10} for propyl (n=3), hexyl (n=6) and decyl (n=10), respectively.

Figure 4.27 depicts the thickness of PMPC brushes grown from silicon-supported mixed tris(TMS)/∝-bromoisobutyrate monolayer having 82%tris(TMS)

coverage. The density of surface-tethered initiator was varied a function of grafting time in the range of 1–4 days. Polymerization was then conducted in methanol using [MPC] = 0.08 M for 5 h in the presence of added initiator. Having similar graft density of initiator (using the same grafting time), the thicknesses of PMPC brushes grown from n_6 and n_{10} are higher than that of PMPC brushes grown from n_3. This outcome can possibly be rationalized as the better mobility and the longer alkyl spacer of n_6 and n_{10} allowing them to conquer the steric hindrance of the surrounding tris(TMS) and reach monomers more efficiently than n_3. It should be noted that the thicknesses of silicon-supported $\propto$-bromoisobutyrate monolayer of n_6 and n_{10} are 15 Å and 18 Å, respectively. It can also be observed that the higher graft density or the longer grafting time of initiator, the denser and the thicker PMPC brushes.
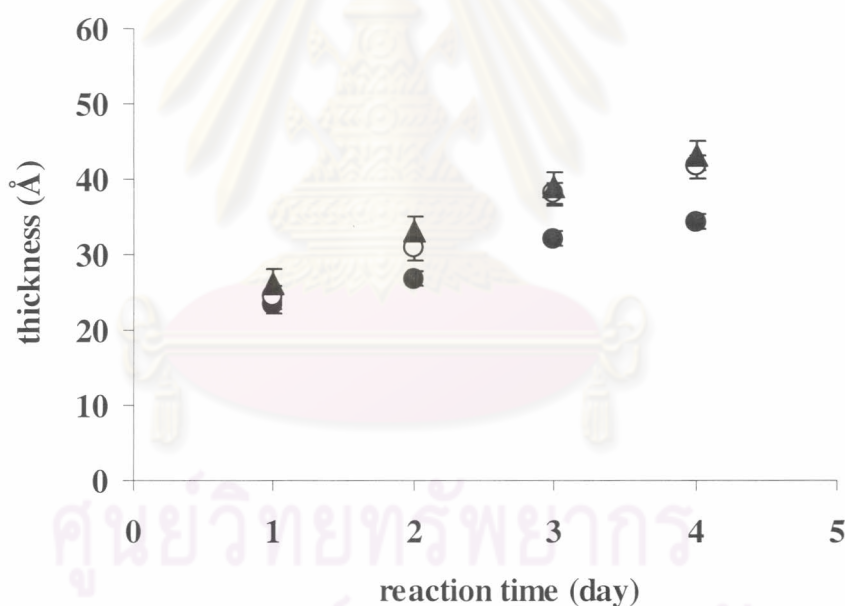
Figure 4.27 Ellipsometric thickness of PMPC brushes grown from silicon-supported mixed tris(TMS)/$\propto$-bromoisobutyrate monolayer having 82% tris(TMS) coverage versus grafting time of initiator in methanol for 5 h: n_3 (●), n_6 (○) and n_{10} (▲).

Using the grafting time of 4 days for all three initiators, the kinetics of surface-initiated polymerization of MPC on silicon-supported mixed tris(TMS)/$\propto$-bromoisobutyrate monolayer (as n_3, n_6, and n_{10}) having 82% tris(TMS) coverage

were determined. The thickness of PMPC brushes as a function of polymerization time is depicted in Figure 4.28. These data clearly suggested that not only does the alkyl spacer influence the ability of $\propto$-bromoisobutyrate to react with monomer but also how fast it can react. The data points at 1h can distinguish the kinetics between n_6, and n_{10} at an early stage of polymerization. Nonetheless, such dissimilarity is no longer noticeable at a later at a longer polymerization time.
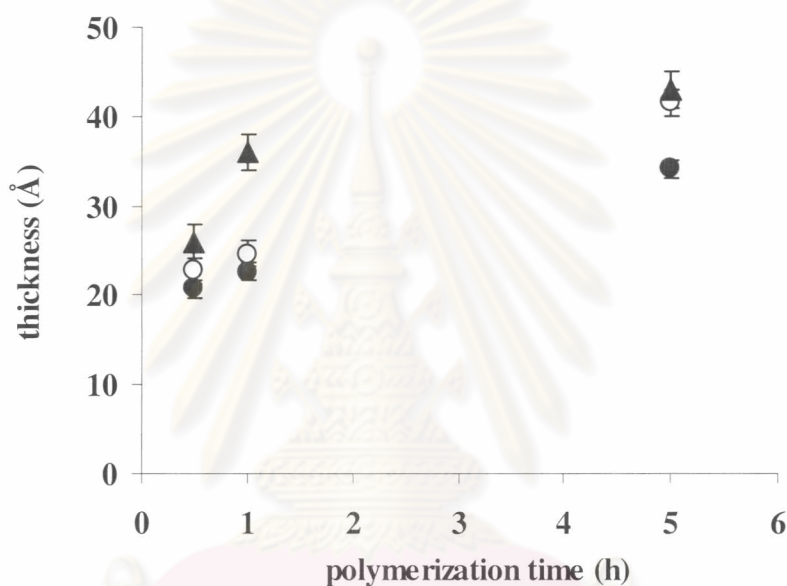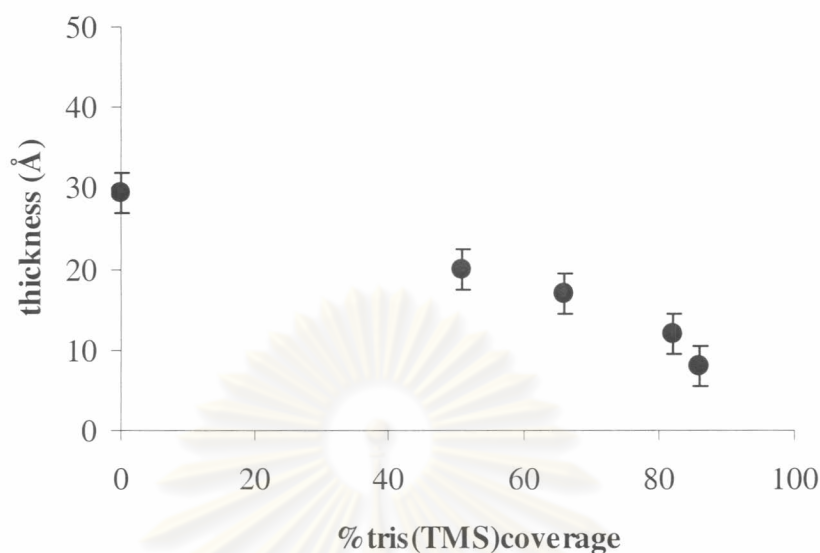

Figure 4.28 Ellipsometric thickness of PMPC brushes grown from silicon-supported mixed tris(TMS)/$\propto$-bromoisobutyrate monolayer having 82%tris(TMS) coverage versus polymerization time in methanol : n_3 ($\bullet$), n_6 ($\circ$) and n_{10} ($\blacktriangle$).
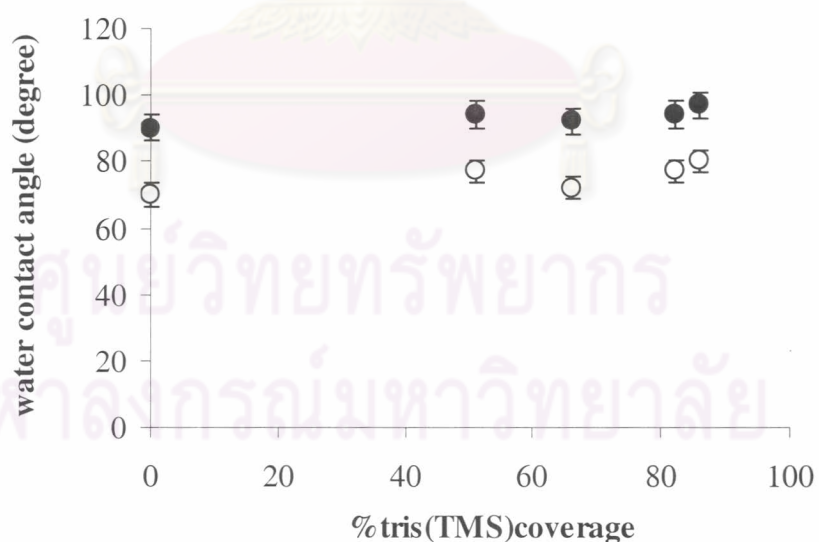
4.4.4 Surface-initiated Polymerization of *t*-BMA from Silicon-supported Mixed Tris(TMS)/∝-Bromoisobutyrate Monolayer

silicon-supported mixed
tris(TMS) / α-bromoisobutyrate monolayer

t-BMA monomer

CuBr/PMDETA

P*t*BMA brush on silicon-supported
mixed tris(TMS) / α-bromoisobutyrate monolayer
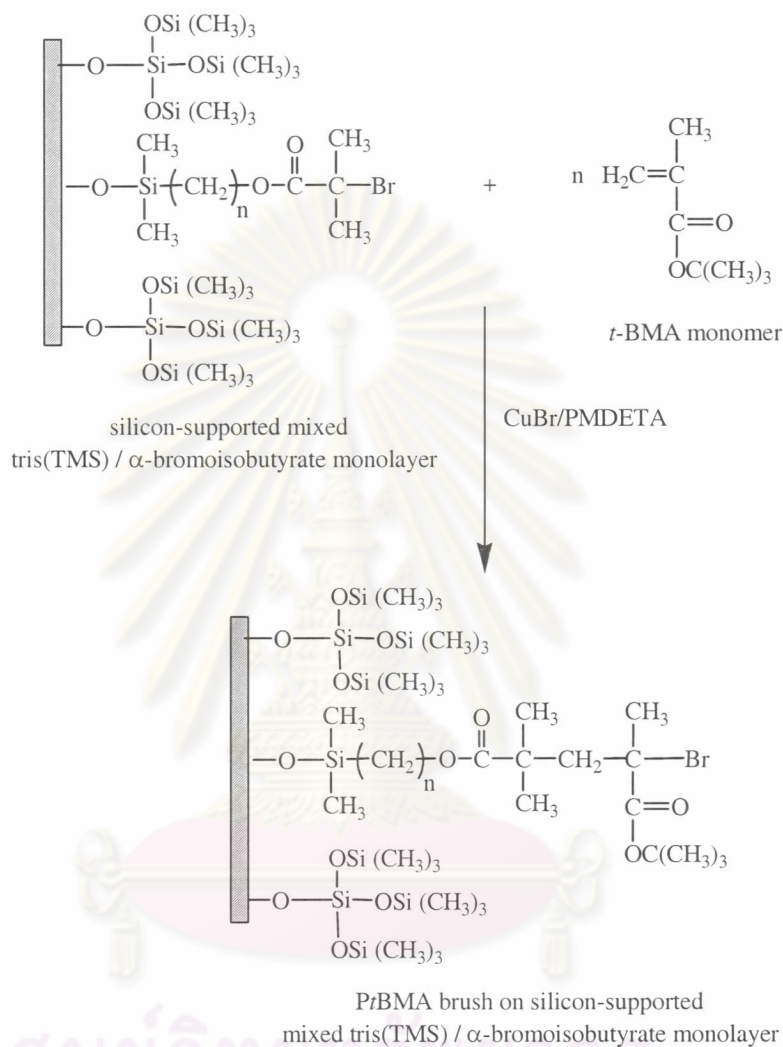
The thickness of grafted P*t*-BMA brushes on tris(TMS)/α-bromoisobutyrate monolayer from toluene is shown in Figure 4.29. The thickness of the grafted polymer layer decreases with increasing tris(TMS) coverage. Figure 4.30 showed that the water contact angles measured on the grafted P*t*-BMA brushes on tris(TMS)/α-bromoisobutyrate monolayer were very close to the value for the homopolymer brush P*t*-BMA (90° / 70°) independent of % tris (TMS) coverage.

Figure 4.29 The thickness of P*t*-BMA brushes grown from silicon-supported mixed tris(TMS)/∝-bromoisobutyrate monolayer using toluene as a solvent for 5 h of polymerization time.

Figure 4.30 Water contact angle of P*t*-BMA brushes grown from silicon-supported mixed tris(TMS)/∝-bromoisobutyrate monolayer using toluene as a solvent for 5 h: of polymerization time θ_A (●) and θ_R (○).

4.5 Surface Topography of Polymer Brushes

AFM was used to study in detail the surface topography of the grafted PMPC brushes on silicon-supported mixed tris(TMS)/∝-bromoisobutyrate monolayer. Figure 4.31 shows AFM images for a clean silicon surface, silicon-supported mixed tris(TMS)/silanol monolayers and their corresponding silicon-supported mixed tris(TMS)/α-bromoisobutyrate monolayers having various percentages of the tris(TMS) coverage. In comparison to a clean substrate, the modified surfaces bearing tris(TMS)/silanol monolayer were almost featureless and relatively smooth. Average roughnesses (Ra) of all modified substrates are listed in Table 4.6. Evidently, neither the coverage of tris(TMS) alone nor the coverage of tris(TMS) and α-bromoisobutyrate significantly altered overall surface roughness.

Table 4.6 Average roughness (R_a) of silicon-supported mixed surfaces determined by AFM analysis.

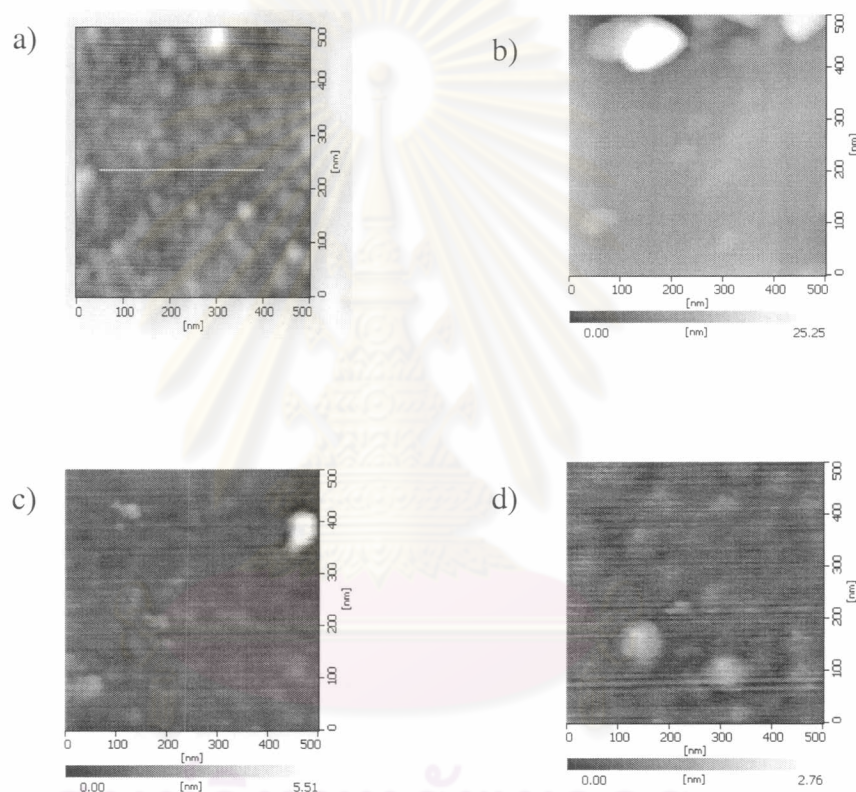| %tris(TMS) coverage	R_a (nm)	
	silicon-supported mixed tris(TMS)/silanol monolayer	silicon-supported mixed tris(TMS)/α-bromoisobutyrate monolayer
0	0.2006	0.1708
51	0.0794	0.1322
66	0.1174	0.1401
82	0.0954	0.1508
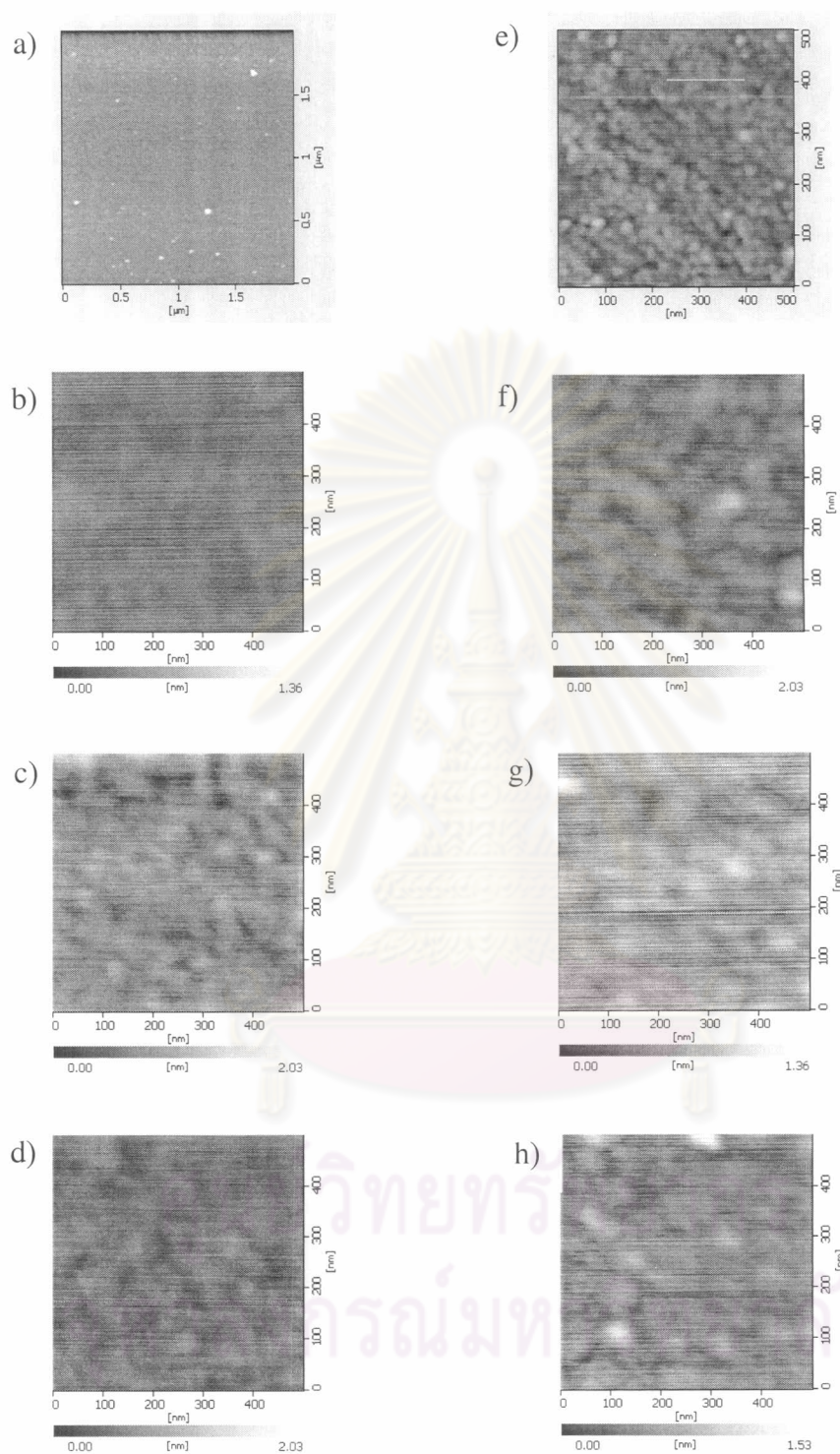
Figure 4.31 AFM images of silicon-supported mixed tris(TMS)/silanol monolayer having varied %tris(TMS) coverage: (a) 0 %, (b) 51%, (c) 66 %, and (d) 82% and silicon-supported mixed tris(TMS)/ α-bromoisobutyrate monolayer having varied %tris(TMS) coverage: (e) 0 %, (f) 51%, (g) 66 %, and (h) 82 %

In order to investigate the spatial distribution of PMPC brushes, silicon-supported mixed tris(TMS)/silanol surfaces having various percentages of the tris(TMS) coverage were used as nano-scale templates for surface-initiated polymerization. The graft density of surface-tethered ∞-bromoisobutyrate groups was also varied as a function of reaction time (1-4 days) between the residual silanol groups in nanopores with the silane compound having end-functionalized α-bromoisobutyrate groups (n_3). The polymerization was mostly conducted in pure methanol. In some cases, we also attempted to grow PMPC brushes in mixed methanol:water = 4:1 (v/v).

Firstly, an effect of %tris(TMS) coverage on topography of surfaces having grafted PMPC brushes was explored. Using 4 days of reaction between silicon-supported mixed tris(TMS)/silanol monolayers and the silane compound having end-functionalized α-bromoisobutyrate groups (n_3), it was assumed that the residual silanols in nanopores are completely replaced by the α-bromoisobutyrate groups that are capable of initiating polymerization. In another word, the nanopores are mostly filled with surface-tethered initiator and there was not much space between the grafted initiators and the surrounding tris(TMS) groups. Originally, we envisioned that protrusions representing the aggregates of PMPC brushes in the nanopores should appear on the surfaces. The higher the %tris(TMS) coverage, the smaller the size of protrusions. AFM images of the silicon-supported mixed tris(TMS)/PMPC brushes having different %tris(TMS) coverage using the polymerization time of 1h in methanol shown in Figure 4.32 suggested otherwise. All surfaces did not show any features that can be evidences of nanoscopic distribution of PMPC brushes grown from the nanopores. According to the data in Table 4.7, the surfaces become even smoother after a longer period of polymerization was used.

It was postulated that the densely grafted PMPC brushes within the limited space in nanopores may be forced by the surrounding tris(TMS) to stretch away from the surface when the polymer chain was relatively short and densely packed inside the nanopores. Under sufficiently long period of polymerization, the polymer chains became so long that they can no longer stretch out, thereby tend to fold over the

tris(TMS) monolayer. For that reason, the surface presumes relatively smooth topography despite of its low overall graft density in the presence of tris(TMS). That was exactly observed in Figure 4.32. Nonetheless, the surfaces may become increasingly rough if the extensive growth of polymer brushes was allowed (polymerization time > 5 h).

Figure 4.32 AFM images of silicon-supported mixed tris(TMS)/PMPC brushes prepared in methanol for 1 h having varied %tris(TMS) coverage : (a) 0%, (b) 51%, (c) 66% and (d) 82%.

Table 4.7 Average roughness (R_a) of silicon-supported mixed tris(TMS)/ PMPC brushes prepared in methanol determined by AFM analysis
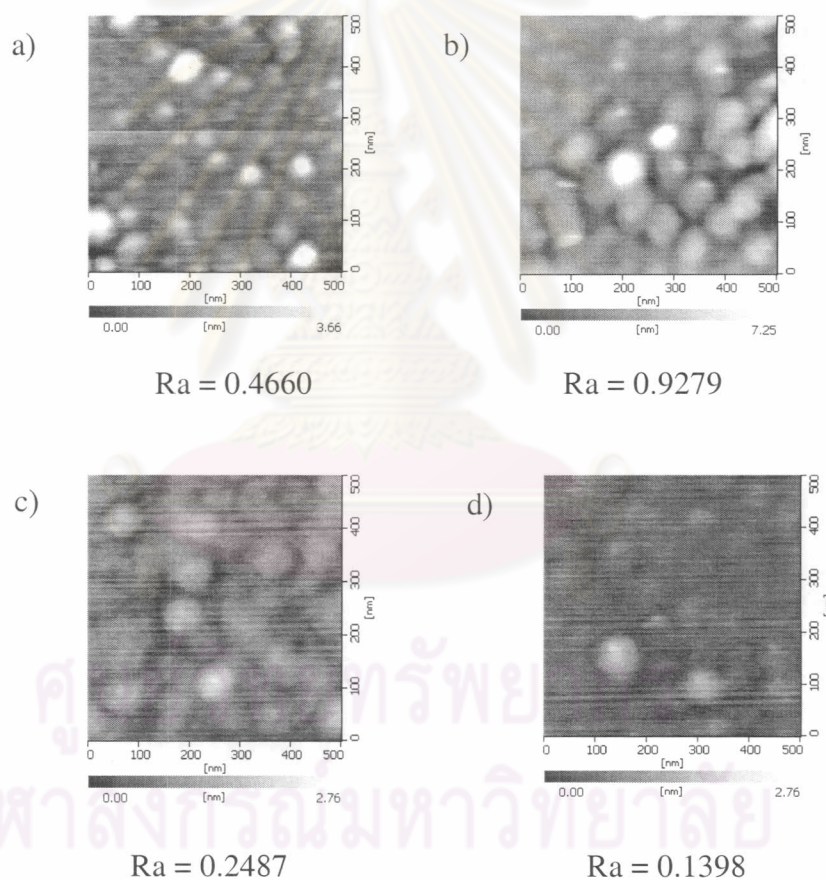
% tris(TMS) coverage	R_a (nm)	
	Polymerization time of 1h	Polymerization time of 5h
0	0.1783	0.1322
51	0.4660	0.1598
66	0.2359	0.1727
82	0.1398	0.1404

To visualize the evolution of PMPC brushes grown from nanopores, two alternative routes were undertaken in order to regulate the graft density of PMPC brushes. Firstly, by fixing %tris(TMS) coverage at 82%, the strategy exploited the kinetics control over the reaction between silicon-supported mixed tris(TMS)/silanol monolayers and the silane compound from 1 to 4 days which later yielded low to high graft density of initiator and corresponding PMPC brushes.

According to Figure 4.33, it was found that the surfaces having varied graft density of PMPC brushes exhibited protrusions having a diameter of less than 100 nm. The size of protrusion was in good agreement with the average roughness (R_a) listed under each images. The protrusions are believed to represent self-aggregation of PMPC brushes in nanopores. In the case of low graft density (Figure 4.33 (a)), there should be enough space within the pores for the polymer chains to adopt more coil-like architecture or aggregated form instead of being in extended forms which are thermodynamically unfavorable. As the packing of PMPC brushes (Figure 4.33 (b)) was denser, the protrusions became larger and so did the roughness.

The surfaces whose nanopores were almost completely covered with PMPC brushes were quite smooth and the protrusions simultaneously diminished as can be

observed in Figure 4.33 (c-d). Such behavior might stem from the fact that PMPC brushes were dense enough to be able to fill the nanopores and to eliminate the valley-and-hill features on the surface. The disappearance of the protrusions may be facilitated by two possible actions of polymer brushes previously explained. The first action involves the polymer chains being forced to stretch away from the surface and thus covering the nanopores while the other involves the folding of polymer chains over the tris(TMS) layer. This latter action should be favorable only when the polymer chains are sufficiently long. Behavior of PMPC brushes can be schematically concluded in Figure 4.34.

a)

Ra = 0.4660

b)
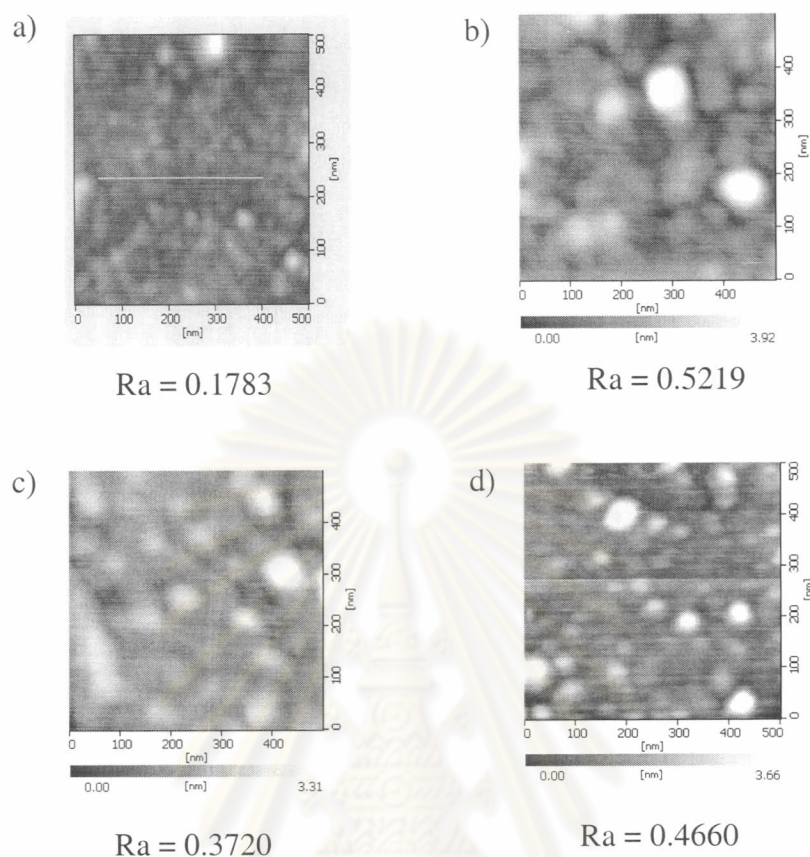
Ra = 0.9279

c)

Ra = 0.2487

d)

Ra = 0.1398

Figure 4.33 AFM images of silicon-supported mixed tris(TMS)/PMPC brushes having 82% tris(TMS) coverage prepared in methanol for 1 h by controlling grafting time of initiator: (a) 1 day, (b) 2 days, (c) 3 days and (d) 4 days.

low graft density   high graft density
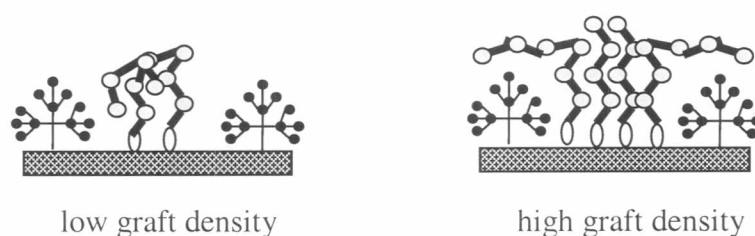
Figure 4.34 Schematic representation of possible orientation of polymer brushes grown from nanopores having different graft densities.

Since the density of PMPC brushes in nanopores is the key to the ability to visualize the polymer distribution, the second alternative route was then done by varying %tris(TMS) coverage, using a short reaction time (1 day) between silicon-supported mixed tris(TMS)/silanol monolayers and the silane compound. These experiments were designed in order to make sure that the residual silanols in nanopores were not completely replaced by the α-bromoisobutyrate groups and these were some space between the grafted PMPC brushes and the surrounding tris(TMS). After the formation of polymer brushes, there should be some space for PMPC brushes to aggregate inside the nanopores. AFM images of silicon-supported mixed tris(TMS)/PMPC brushes prepared by this approach are illustrated in Figure 4.35. The size of protrusions obviously reflected the size of nanopores which should be inversely proportional to %tris(TMS) coverage. The higher %tris(TMS) coverage, the smaller the protrusions.

Ra = 0.1783   Ra = 0.5219

Ra = 0.3720   Ra = 0.4660

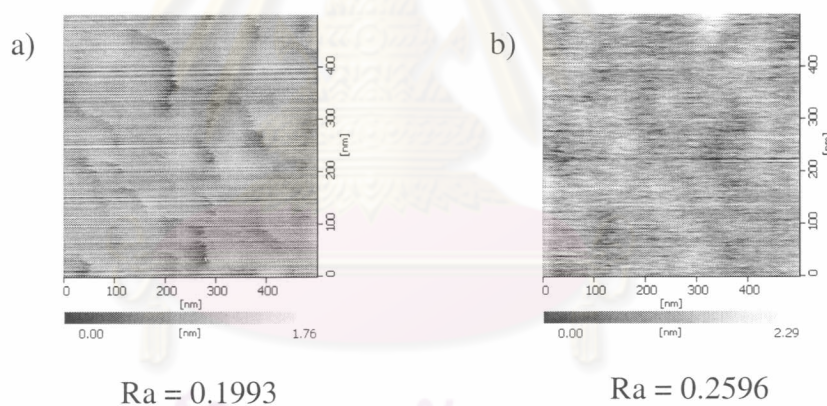**Figure 4.35** AFM images of silicon-supported mixed tris(TMS)/PMPC brushes prepared in methanol for 1 h using grafting time of initiator (n_3) for 1 day and having varied % tris(TMS) coverage: (a) 0%, (b) 51%, (c) 66% and (d) 82%.
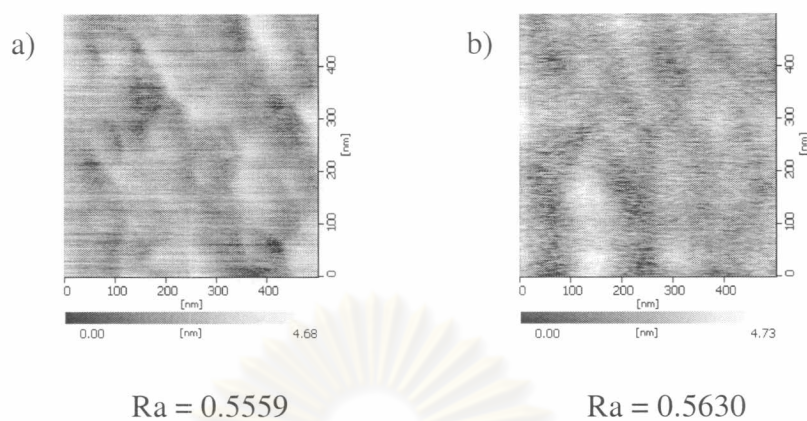
Comparative investigation has been conducted on the system of silicon-supported mixed tris(TMS)/Pt-BMA brushes. Figure 4.36 shows AFM images of silicon-supported mixed tris(TMS)/Pt-BMA brushes having 82% tris(TMS) coverage. Pt-BMA brushes was grown in toluene for 1 h from silicon-supported mixed tris(TMS)/α-bromoisobutyrate having different graft densities of α-bromoisobutyrate groups. Conducting the reaction between silicon-supported mixed tris(TMS)/silanol monolayers and silane compound having end-functionalized α-bromoisobutyrate groups (n_3) for 1 day and 4 days yielded low and high graft density of α-bromoisobutyrate groups, respectively. Even though both surfaces have different graft densities of Pt-BMA brushes, their surface topographies are

indistinguishable and relatively smooth in texture. The surfaces became rougher when polymerization time was extended from 1h to 5h (Figure 4.37) without affecting surface topographies. Unlike PMPC brushes, P*t*-BMA brushes are hydrophobic. Therefore, they should be quite miscible with tris(TMS). In fact, this speculation can be confirmed by contact angle data shown in Figure 4.30. The mixed tris(TMS)/P*t*-BMA brush system thereby did not exhibit nanoscopic phase separation although the surface graft density of P*t*-BMA brushes was low. These results also implies that self-aggregation of PMPC brushes in nanopores which appears as protrusions is truly a consequence of phase incompatibility between hydrophilic PMPC brushes and hydrophobic tris(TMS). Once again, it should be highlighted that such nanoscopic phase separation was noticeable when graft density of PMPC brushes was low.

Ra = 0.1993   Ra = 0.2596

Figure 4.36 AFM images of silicon-supported mixed tris(TMS)/PtBMA brushes having 82% tris(TMS) coverage prepared in toluene at 90 °C for 1 h by controlling grafting time of initiator: (a) 1 day and (b) 4 days.

a)   b)

Ra = 0.5559   Ra = 0.5630

Figure 4.37 AFM images of silicon-supported mixed tris(TMS)/PtBMA brushes having 82% tris(TMS) coverage prepared in toluene at 90 °C for 5 h by controlling grafting time of initiator: (a) 1 day and (b) 4 days.